An engineering study on the enhanced control and operation of continuous manufacturing of pharmaceutical tablets via roller compaction

Ravendra Singh, Marianthi Ierapetritou, Rohit Ramachandran*

Engineering Research Center for Structured Organic Particulate Systems (ERC-SOPS), Department of Chemical and Biochemical Engineering, Rutgers, The State University of New Jersey, Piscataway, NJ 08854, USA

ARTICLE INFO

ABSTRACT

A novel manufacturing strategy based on continuous processing integrated with online monitoring tools coupled with efficient automatic feedback control system is highly desired for efficient Quality by Design (QbD) based manufacturing of the next generation of pharmaceutical products with optimal consumption of time, space and resources. In this manuscript, an efficient plant-wide control strategy for an integrated continuous pharmaceutical tablet manufacturing process via roller compaction has been designed in silico. The designed control system consists of five cascade control loops and three single control loops resulting in 42 controller tuning parameters. An effective controller parameter tuning strategy involving an ITAE method coupled with an optimization strategy has been proposed and the designed control system has been implemented in a first principle model-based flowsheet that was simulated in gPROMS (Process System Enterprise). The advanced techniques (e.g. anti-windup) have been employed to improve the performance of the control system. The ability of the control system to reject the unknown disturbances as well as to track the set point has been analyzed. Results demonstrated enhanced performance of critical quality attributes (CQAs) under closed-loop control compared to open-loop operation thus illustrating the potential of closed-loop feedback control in improving pharmaceutical manufacturing operations.

1. Introduction

Pharmaceutical industries are facing enormous challenges to satisfy regulatory constraints, flexible market demands, operational complexities and economical limitations. Because of globalization, the patents' life of new discovered drugs has also been decreased considerably forcing the manufacturer to minimize the drug development time as well as maximize the throughput and for this, continuous manufacturing has evolved as an efficient alternative (Singh et al., 2011). However, better process understanding and control are vital to minimize the product waste due to manufacturing failure and produce product of desired quality with reduced end product testing (Charoo et al., 2012). Therefore, a significant opportunity exists to improve the product quality and to optimize the production process through the implementation of innovative solutions for on-line monitoring, analysis and system control (Singh et al., 2009). The US food and drug administration (FDA/CDER, 2005) have taken an initiative for application of Process Analytical Technology (PAT) and control system to the manufacturing industries. Application of PAT systems (FDA/CDER, 2005) in manufacturing

paves the way for continuous process and product improvements through improved process supervision based on knowledge-based data analysis, 'Quality by design (QbD)' concepts, and through feedback control (Gnoth et al., 2007). The primary goal of PAT is to better understand the manufacturing process, and to use that knowledge on-line to achieve better control of the process and thus consistent product quality. PAT is therefore defined as a system for designing, analyzing, and controlling manufacturing through timely measurements (i.e., during processing) of critical quality and performance attributes of raw and in-process materials and processes with the goal of ensuring final product quality (FDA, 2004; FDA/CDER, 2005).

Automated continuous processes coupled with efficient feedback control systems are highly desired for pharmaceutical production due to high efficiency, enhanced product quality, and less need of space, labor and resources. However, in the past, the pharmaceutical industry has been hesitant to introduce innovative systems into the manufacturing sector for several reasons. One often cited reason is regulatory uncertainty, which may result from the perception that the existing regulatory system is rigid and unfavorable to the introduction of innovative systems (FDA, 2004; Plumb, 2005). As a consequence, the pharmaceutical industry is still dominated by batch processes with the mindset that products can only be produced by batch processes or a 'frozen' manufacturing system, if they are to comply with regulatory quality

* Corresponding author. Tel.: +1 7324456278; fax: +1 7324452581.
  E-mail address: rohit.r@rutgers.edu (R. Ramachandran).

Nomenclature

A	surface area [m^2]
C_{API}	API Composition
d_{50}	mean particle size [m]
F	PBM density function [particles]
H	height [m]
h_0	half of ribbon thickness [m]
m	mass flow [kg]
n	number
P	compaction pressure [MPa]
R	radius [m]
RSD	Relative Standard Deviation
RT	residence time [s]
u	feed speed [m/s]
W	width [m]
α	nip angle [radians]
δ	effective angle of friction [radians]
ε	porosity
θ_{in}	inlet angle [radians]
ρ_{bulk}	powder bulk density [kg/m^3]
σ	material stress [MPa]
$\Re$	rate [particles/s]
ω	feeder rotation rate [rpm]
C_1^{rc}	stress-angle empirical parameter
k_{break}	breakage kernel
K^{rc}	stress-angle empirical parameter
θ	delay
τ	time constant

Domain

g	gas
n	component
r	particle size
s_1	API
s_2	excipient
z	time delay
z_1	axial
z_2	radial

subscript

in	inlet stream
out	outlet stream
P	pressure
set point	sp
u	speed
ω	rotation rate

superscript

delayed	delayed
disc	feed frame disc
f	feeder
ff	feed frame
m	mixer
mil	mill
rc	roller compactor
rib	ribbon
rol	roller compactor roll
tp	tablet press

labor intensive. However, one major advantage of batch processing is flexibility. Flexibility means that the same equipment can be used to fulfill more than one purpose. Efforts are being made in order to render significant flexibility to the continuous processes as well (Singh et al., 2011, 2012). There is now a window of opportunity for the pharmaceutical industry to change the mind-set and move towards new innovative manufacturing concepts. Continuous manufacturing processes – naturally eliminating the batch processing drawbacks – have a major potential to provide an alternative. There are many other examples in the scientific literature, where a need to move from batch to innovative continuous processing is encouraged (e.g. Baumann et al., 2008; Betz et al., 2003; Buchholz et al., 2010; Lomel et al., 2006; Malhotra, 2009; Plumb, 2005; Saaby et al., 2005; Schaber et al., 2011; Sedelmeier et al., 2009; Stitt, 2002; Trout, 2007; Watts and Haswell, 2003; Wheeler, 2009). This clearly indicates that there is currently an environment in which pharmaceutical companies can start to consider changes to their processes, but significant cultural change is still required (Lamb et al., 2010).

In the last few years, very few attempts have been made toward the control of a tablet manufacturing process. Ramachandran and Chaudhury (2012) have proposed a control system for a continuous drum granulation process, an important unit operation used for wet granulated continuous tablet manufacturing process. Hsu et al. (2010a, 2010b) have suggested a control system for a roller compactor, an important unit operation used for dry granulated continuous tablet manufacturing process. However, a satisfactory control performance has not been achieved. Ramachandran et al. (2012) have designed a control system for a direct compaction process with emphasis on blending and tableting process. Singh et al. (2010a) have suggested a monitoring and control system for a batch tablet manufacturing process. However, no attempt has been made to design a control system for an integrated continuous tablet manufacturing process with dry granulation (using roller compaction).

In this manuscript an efficient control system for an integrated continuous pharmaceutical tablet manufacturing process with roller compaction has been designed. The designed control system has been implemented in a first principle model simulated in a simulation tool (gPROMS, Process System Enterprise). A dynamic optimization method has been used to tune the controller parameters. The systematic application of the control system can enable the manufacturer to achieve the predefined end product quality consistently.

2. Systematic framework for the design of an efficient process control system

The design and implementation of an efficient process control system is an interactive procedure that involves the identification of critical controlled variables, coupling of the controlled variables with suitable actuators (manipulated variables), selection of suitable monitoring tools, selection of control strategy followed by tuning of controller parameters, model-based closed-loop performance assessment, and finally implementation to the manufacturing plant through the available sensing and control hardware (e.g. Delta V, Emerson) and control interface (e.g. OLE Process Control (OPC)). A systematic framework for design and implementation of an efficient control system is shown in Fig. 1. The design methodology consists of 12 hierarchical steps. The first step is concerned with specifying the product properties that are desired to be achieved in the considered production process. The necessary process relates information, such as the raw materials, their composition and the equipments used in the production process are provided in step 2 (process specifications). The information provided through these two steps of the design methodology act
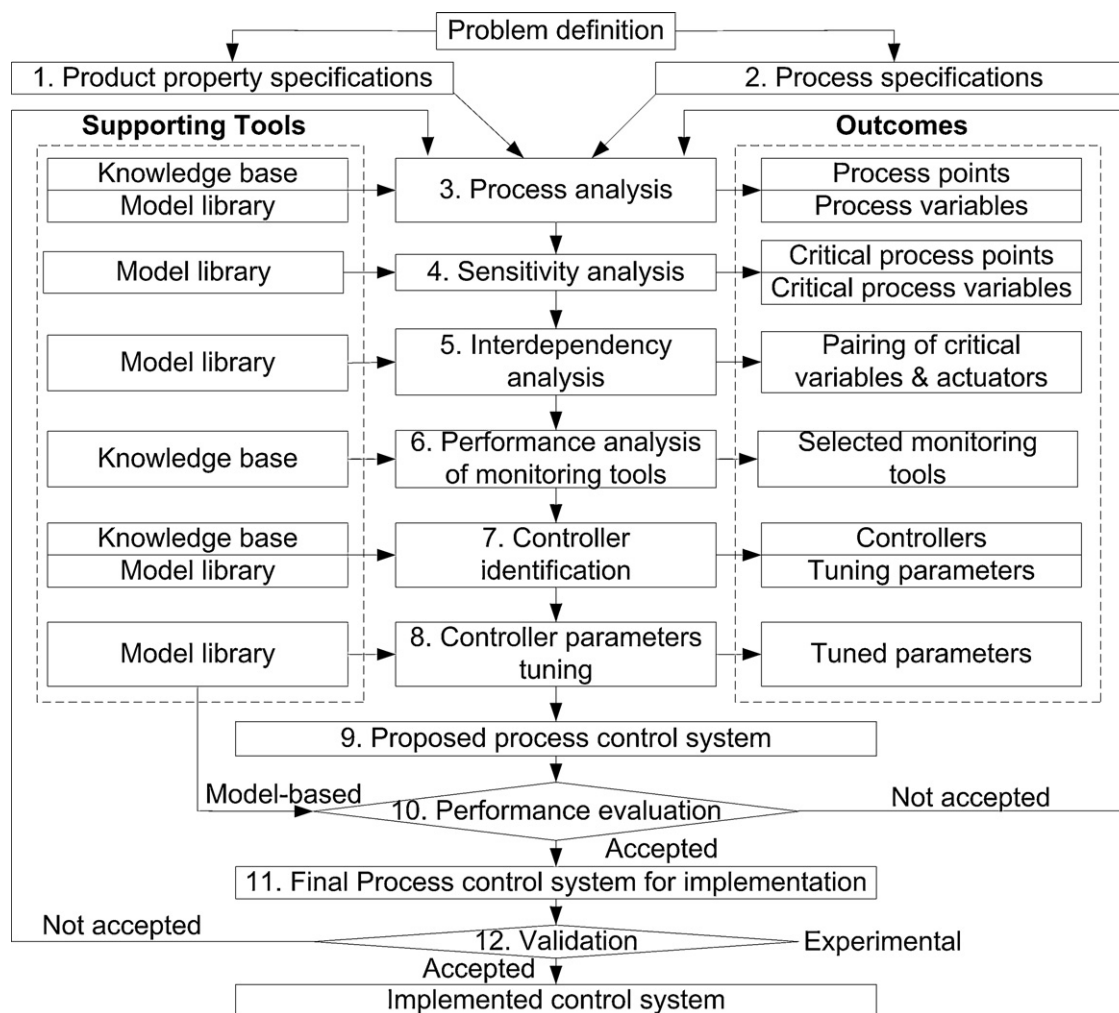
requirements (Plumb, 2005). In fact, batch processes are not particularly good for product quality assurance and possess a number of drawbacks such as poor process understanding, yield, scalability, and energy inefficient. In addition, batch processes are also

Fig. 1. Systematic framework for design and implementation of control system (extended from Singh et al., 2009).

as input data for the design problem. On the basis of the input data and with the consultation of the knowledge base, step 3 (process analysis) of the methodology generates a list of process points (in general, process equipments are considered as the process points) and a list of the corresponding process variables. The outcome of this step becomes the basis for subsequent analysis steps. The critical process points where monitoring and analysis equipments need to be placed and the corresponding critical process variables that need to be monitored and controlled in order to achieve the desired end product quality are then identified through step 4 (sensitivity analysis). The identification of the appropriate actuators and the selection of suitable on-line monitoring techniques and tools are necessary to successfully implement the control system in order to control the critical process variables obtained in step 4. The appropriate actuator for each selected critical process variable is identified through step 5 (interdependency analysis) while step 6 (performance analysis of monitoring tools) generates the list of the feasible measurement methods and tools for selected critical process variables (Singh et al., 2010b, 2009). The suitable controller for each controlled variable is then selected in step 7. Depending on the dynamic response of the process, either basic controllers (e.g. Proportional Integral Derivative (PID)) or advanced controller (e.g. Model Predictive Controller (MPC)) can be selected. After deciding the type of controllers the corresponding control parameters that need to be tuned can be listed. For example, if the controller selected is PID then the parameters that need to be tuned are gain (K_C), reset time (K_I) and rate (K_D). In step 8, all the control parameters need to

be tuned for that heuristic methods (e.g. Ziegler Nichols method) or optimization based method (e.g. ITAE: Integral of Time Absolute Error) can be used. On the basis of the outcomes of steps 4–8, a control system is suggested in step 9. The proposed control system consists of a list of critical process points, corresponding critical process variables, actuators, monitoring techniques and monitoring tools, controllers and corresponding controller parameters. The control system is then implemented in a mathematical model to evaluate its performance (step 10). If the performance is found to be satisfactory then the final control system is proposed in step 11 that can be implemented in the plant for experiment based performance evaluation and plant operation (step 12). The supporting tools and corresponding outcomes are also highlighted in the figure. An integrated mathematic model for continuous tablet manufacturing process that used for design of control system is a part of model library. The model is given in Appendix A. The knowledge base consist the information about the process as well as the information about the monitoring and control system. The application of the knowledge base is demonstrated elsewhere (Singh et al., 2010b).

3. Continuous tablet manufacturing process

3.1. Process description

The process considered for the design of a control system is a pilot plant for continuous tablet manufacturing process situated at the Engineering Research Center for Structured Organic Particulate
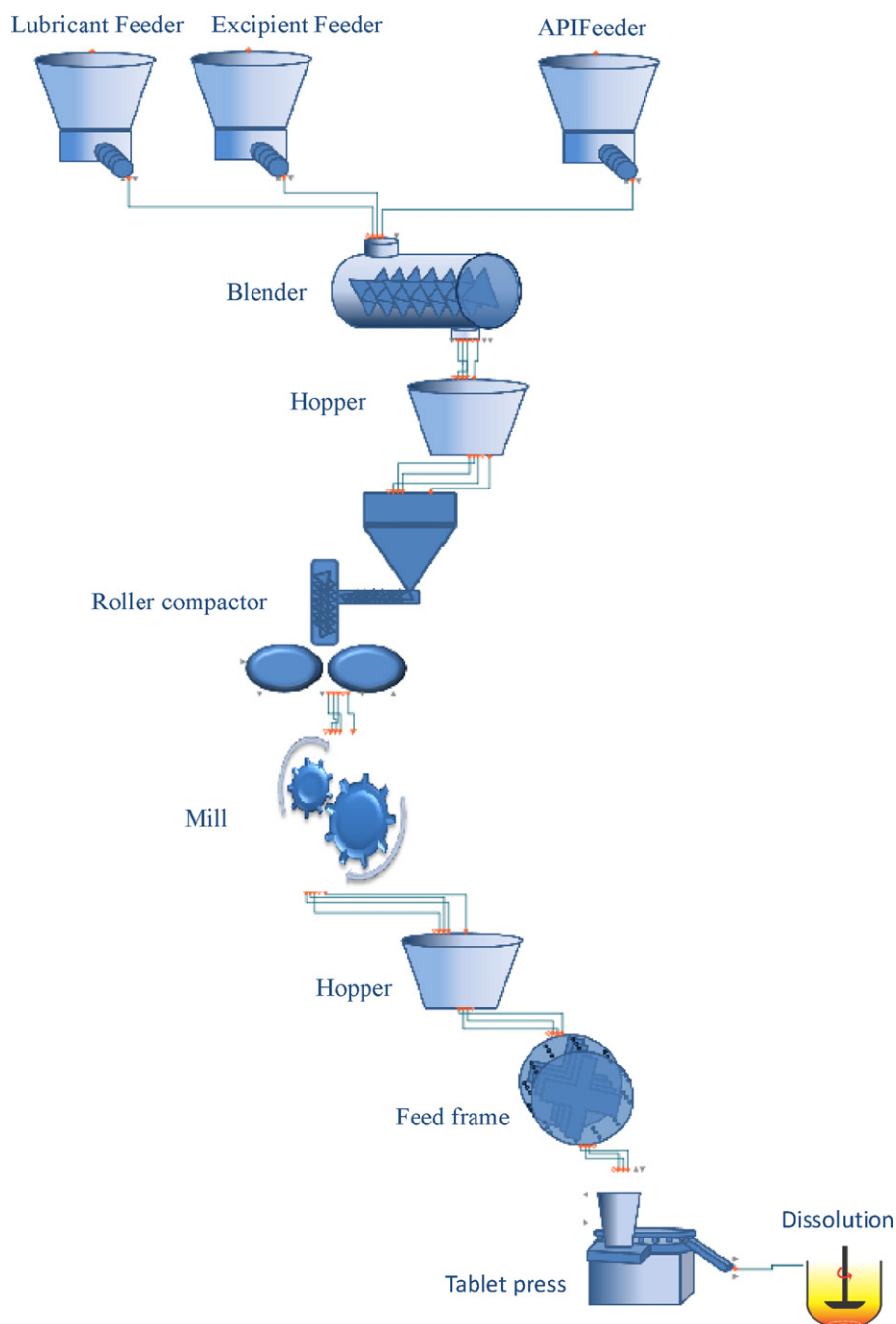
Fig. 2. Schematic of a continuous tablet manufacturing process via roller compaction.

Systems (ERC-SOPS), Rutgers University. Some details of the pilot plant have been previously reported (Vanarase and Muzzio, 2011) and the open-loop operation has been extensively studied (Boukouvala et al., 2011, in press; Portillo et al., 2010; Vanarase et al., 2010, 2011). The process flowsheet for continuous tablet manufacturing process is shown in Fig. 2. As shown in the figure, there are three gravimetric feeders to provide necessary lubricant, API and excipient. The feeders itself contain a hopper that can hold up to a certain amount of material and a rotating screw to change the flow rate. These feeds are then fed to a blender to generate a homogeneous mixer. Outlet from the blender is fed to a hopper to maintain a certain amount of the materials that need to flow in roller compactor. Roller compaction is used to make ribbons

from powder blends obtained from the mixer. Roller compactor is a novel unit operation used for dry granulation, particularly suitable for the cases where powder feeds are water sensitive (Hsu et al., 2010a). Ribbons obtained from the roller compactor are then milled to smaller size ranges in a mill (e.g. hammer mill). Oversized particle obtained from the mill can be recycled to the mill while the undersize particle can be recycled to the roller compactor. Desired granules obtained from the milling machine are then sent to a hopper. From the hopper, the powder granules are then sent to a tablet press through a feed frame. Final compacted tablets are then obtained from the tablet press and among them, few tablets can be sent for dissolution testing. The process flowsheet has been implemented into a simulation software gPROMS (Process Systems

Enterprise, http://www.psenterprise.com/). The methodology to develop an integrated process flowsheet has been described in Boukouvala et al. (in press).

3.2. Process models

Extensive research has been undertaken to develop the first principle models of different unit operations involved in the tablet manufacturing process. A summary of some of these process models is previously reported in Boukouvala et al. (in press). The detail developments of these models are reported elsewhere as summarized here. The mathematical model for powder blending, an important but complex unit operation, has been previously developed (Sen and Ramachandran, in press; Sen et al., 2012). The model of roller compactor is adapted from Hsu et al. (2010a, 2010b). The model of tablet compression process is previously reported in Singh et al. (2010a). This model is based on Kawakita powder compression model (Kawakita and Ludde, 1971). The dissolution model is adapted from Kimber et al. (2011). The models of different unit operations have been developed and included in gPROMS library to facilitate the integrated flowsheet modeling. The development of the integrated process flowsheet using individual unit operation models has been previously demonstrated (Boukouvala et al., in press). The controller models have been selected from the control section of the Process Model Library (PML) of simulation software gPROMS. The first principle model, representing the real dynamics of the process, is used to design the control system of continuous tablet manufacturing process. The models used for design of a control system for continuous tablet manufacturing process are given in Appendix A.

4. Design of the process control system

A process control system for the tablet manufacturing process using roller compaction was then designed using the methodology was shown in Fig. 1. The final product specifications include tablet weight, tablet hardness, and tablet dissolution (step 1). The unit operations are shown in Fig. 2. API, Excipient and Lubricant are the important feeds to the process (step 2).

4.1. Main process points and process variables (step 3)

The overview of the main process variables relevant for process control that could potentially influence the end product quality of a pharmaceutical tablet manufacturing process is shown in Fig. 3. Only selected process variables that could potentially influence the end product quality and may be relevant for process control are included in the figure. In principle, most of the variables could have an influence on each other in some extent but not all the process variables can be monitored and controlled. Fig. 3 also shows the complex interaction involved among the variables. For example, feed properties as well as feed flow rates could affect the Relative Standard Deviation (RSD) that in turn could affect the ribbon density that could itself affect the composition uniformity of the granules. Composition uniformity of the granules could affect the API composition of the tablets that finally could affect the physiological properties of the tablets. The process parameters (highlighted with red color and dashed line) are potential actuator candidates while the process variables are potential candidates to be considered for control. The corresponding unit operations are also shown in Fig. 3.

4.2. Critical process controlled variables (step 4)

The process variables that could potentially influence the end product quality, plant safety and operation are considered as the

Table 1
List of controlled variables considered in the overall process.

Critical process points	Critical process variables
Blender	RSD (CQA)
	Total flow rate (CPP)
	AP composition (CQA)
	API Excipient ration (CQA)
Roller compactor	Ribbon density (CQA)
	Throughput (CPP)
Milling	Granule size (CQA)
Tablet press	Tablet weight (CQA)
	Tablet hardness (CQA)
	Tablet thickness (CQA)
	Tablet dissolution (CQA)

critical process variables that are desired to be monitored and controlled throughout the plant operation. Based on experimentation and model based analysis, the critical controlled variables are selected (from the variables shown in Fig. 3) as listed in Table 1 (Hsu et al., 2010a,b; Ramachandran et al., 2012; Singh et al., 2010a). A methodology to identify the critical controlled variables is previously developed (Singh et al., 2009) and implemented into a software (Singh et al., 2010a). CPP (critical process parameter) and CQA (critical quality attribute) of this process as desired buy regularly authority (e.g. FDA) are also indicated in the table.

4.3. Controlled variables and actuators pairing (step 5)

The selection of a suitable actuator for each controlled variable (see Table 1) is essential to achieve satisfactory control loop performance. However, being a highly interactive system, the selection of the right actuator for the continuous tablet manufacturing process is a challenging task. Few potential actuator candidates corresponding to each controlled variables are listed in Table 2. The final actuators are selected based on dynamic sensitivity analysis. The actuator candidates are perturbed and the effect on the controlled variables is analyzed. The actuator candidates that have more effect on controlled variable are more sensitive and therefore can be considered as the suitable actuator. In dynamic sensitivity analysis, the effects of actuator candidates on a controlled variable can be analyzed in whole operational period therefore is better than the methods based on analysis at steady state (e.g. relative gain array method). The blending process is considered here as a demonstrative example for actuator selection. In this process, there are three controlled variables (Total flow rate, RSD, API composition) and three actuator candidates (rotation speed of API feeder, rotation speed of lubricant feeder, rotation speed of blender). The actuator candidates have been perturbed (from +3% to −3% with step size of 1) and the absolute percentage changes in controlled variables have been analyzed.

$$\text{Absolute \% change in controlled variable} = 100 \left| \frac{Y_0^j(t) - Y_i^j(t)}{Y_0^j(t)} \right|$$

where $Y_i^j(t)$ is the value of Controlled variable in ith perturbation of jth actuator candidate and $Y_0^j(t)$ is the base value for the jth actuator candidate.

The effects of actuator candidates on total flow rate (controlled variable) are shown in Fig. 4a. As shown in the figure, at steady state the rotation speed of the feeder that provides the API is much more sensitive in comparison to other two actuator candidates therefore it can be selected as the final actuator. During startup, other actuator candidates also have significant sensitivity on controlled variable that makes the blender process control a difficult task. The sensitivity of the actuator candidates on controlled variable can
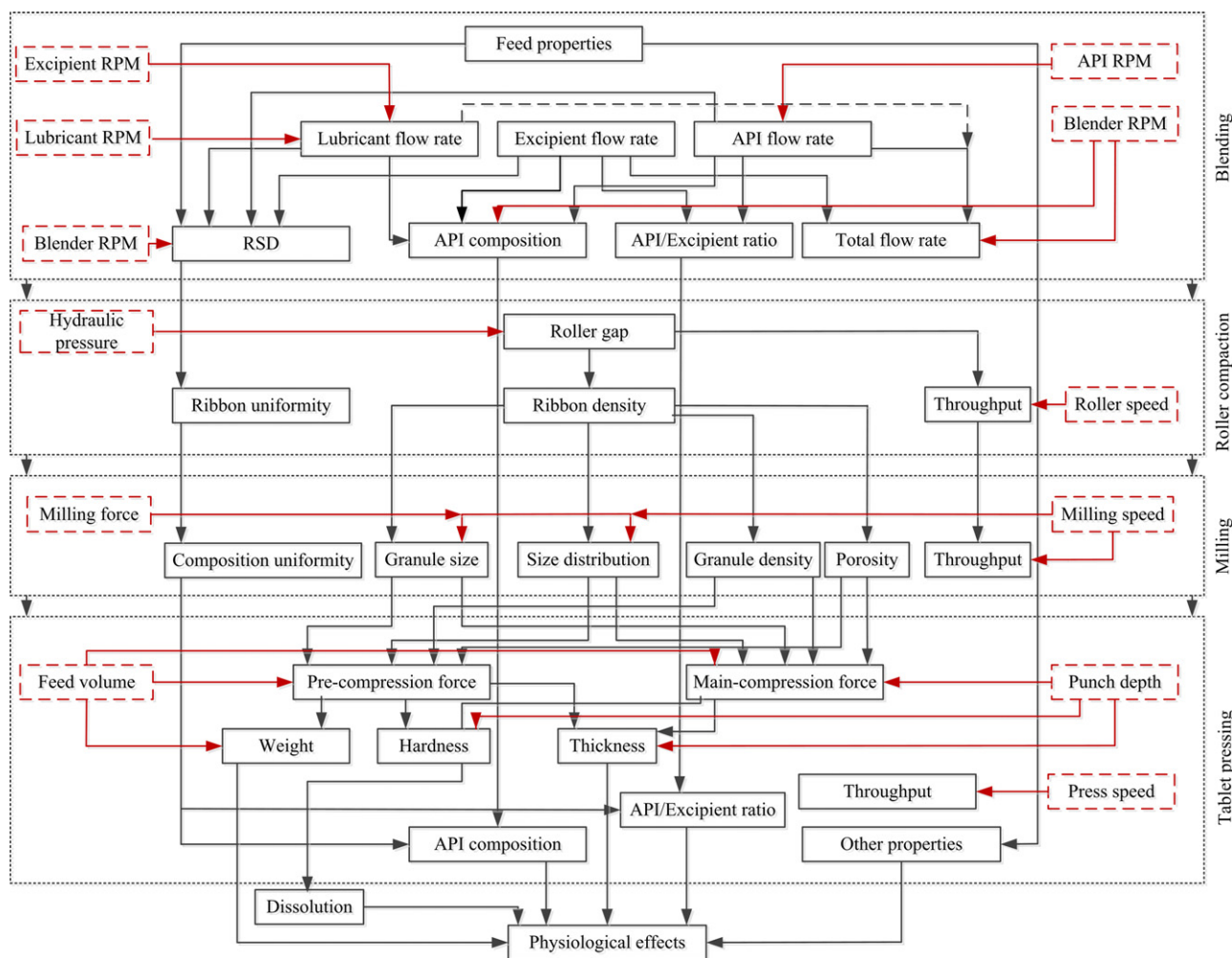
Fig. 3. Overview of the main process variables.

be compared at steady state through a two dimensional projected view as shown in Fig. 4b. It should be noted that API and excipient need to be maintained at certain ratio through a ratio controller therefore on changing the API flow rate the excipient flow rate will also change.

The remaining two controlled variables (RSD and API composition) have two actuator candidates. As shown in Figs. 5 and 6, these two control loops are highly interactive. However, from Fig. 5b it can be concluded that the rotation speed of the blender is a more sensitive actuator candidate at steady state for API composition except at higher value of changes (>2%) therefore it could

be considered as the actuator for the API composition control. Fig. 5a shows that during startup the actuator candidates are much more sensitive in comparison to the steady state. As shown in Fig. 6, the remaining actuator candidate (rotation speed of lubricant feeder) can be used for the control of the relative standard deviation. It should be noted that the sensitivities of the blender and lubricant feeder rotation speeds on API composition and RSD are very small. Therefore, these variables are difficult to control at new set points. However, the minor adjustment on API composition and RSD can be achieved by manipulating the rotation speed of blender and lubricant feeder, respectively. Similarly, the actuator for the

Table 2
Controlled variables and actuators pairing.

Critical process points	Critical process variables	Main actuator candidates
Blender	RSD	Rotation speed of blender, Rotation speed of *lubricant feeder*[a], Rotation speed of API and Excipient feeder
	Total flow rate	Rotation speed of blender, Rotation speed of lubricant feeder, *Rotation speed of API and Excipient feeder*[a]
	API composition	*Rotation speed of blender*[a], Rotation speed of lubricant feeder, Rotation speed of API and Excipient feeder
	API Excipient ratio	*Rotation speed of excipient feeder*[a]
Roller compactor	Ribbon density	*Hydraulic pressure*[a], roller speed
	Throughput	Hydraulic pressure, *roller speed*[a]
Milling	Granule size	*Mill rotation speed*[a], Mill pressure
Tablet press	Tablet weight	*Feed volume*[a], Pre-compression force, Main compression force
	Tablet hardness/Tablet thickness	*Punch displacement*[a], Pre-compression force, Main compression force
	Tablet dissolution	*Punch displacement*[a], Pre-compression force, Main compression force

[a] Identified actuators
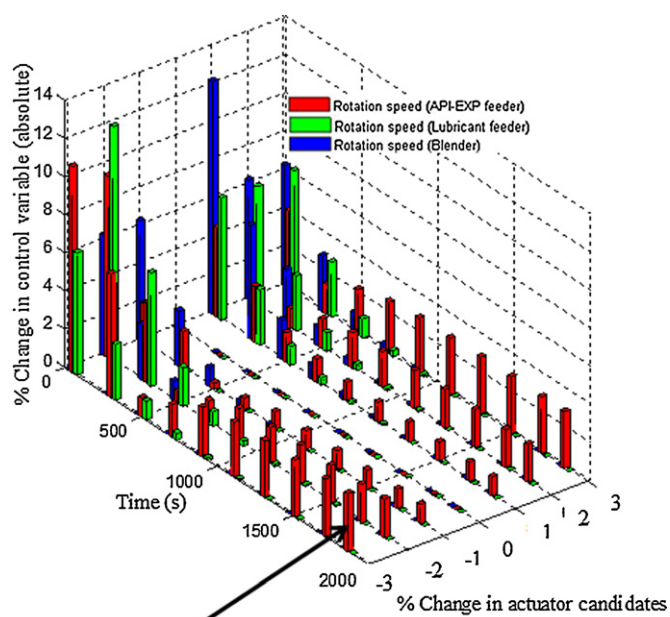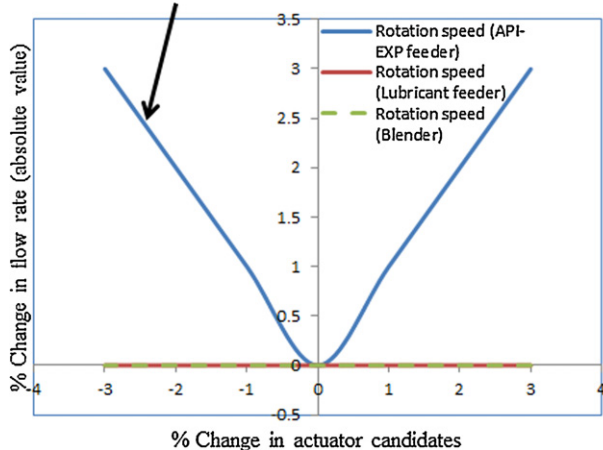
Fig. 4. Selection of actuator for flow rate control: (a) 3D visualization, (b) 2D.

Fig. 5. Selection of actuator for API composition control: (a) 3D visualization, (b) 2D visualization.

other controlled variables has been identified as given in Table 2 (highlighted with italics).

Some variables listed in Table 2 can be controlled directly via a single feedback controller and some variables cannot be controlled directly because of the large time delay involved. The final controller configurations highlighting the type of control system required is given in Table 3. Cascade control systems are proposed for controlling of RSD, Total flow rate from blender, ribbon density, tablet weight and hardness because of larger delay time involved. Cascade control can improve control system performance over single-loop control in many instances, for example when a large time delay is involved, when disturbances affect a measurable intermediate that directly affects the controlled variable, the gain of the secondary process including the actuator is nonlinear. In the proposed cascade control systems, the dynamics of the inner loops are significantly faster than the outer loops indicating that the performance of the cascade control system will be better than a single-loop control system. For other variables the single-loop controllers are sufficient. RSD has been controlled by manipulating the lubricant flow rate and for changing the lubricant flow rate the rotation speed of the lubricant feeder need to be changed in a cascade control scheme. Note that the rotation speed cannot be directly manipulated to control RSD because of the high time
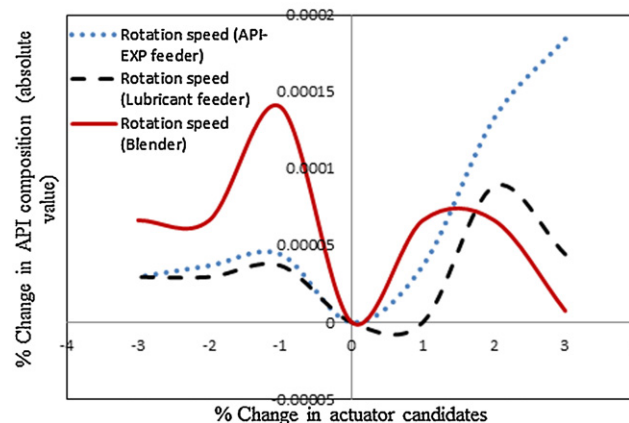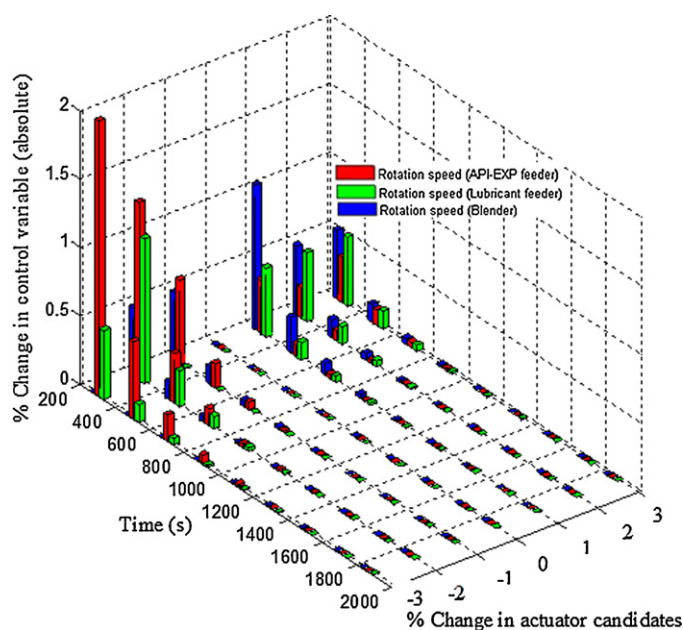
delay involved. Similarly, the total flow rate from the blender is controlled by manipulating the API flow rate that itself has been changed by manipulating the API feeder rotation speed. In roller compactor, ribbon density is controlled by manipulating the roller gap that itself has been changed by manipulating the hydraulic pressure, through a cascade control system. Changing the roller gap will affect the throughput from roller compactor therefore it also need to be controlled by manipulating the roller speed (RPM). In milling process the particle size is controlled by manipulating the mill rotation speed. In the tablet compaction process, tablet weight and hardness could be controlled separately by using the pre-compression force and main compression force. For controlling the tablet weight the pre-compression force has been manipulated that itself has been changed by manipulating the feed volume through a cascade control scheme. Similarly, for desired hardness the main compression force has been manipulated that itself has been changed by manipulating the punch displacement. One of the final product qualities is dissolution that depends on the other variables including tablet hardness. However, maintaining a consistent hardness does not guarantee a consistent dissolution because dissolution depends on other process variables and material attributes as well. For example, particle size and bulk density of the feed powder, API/Excipient ration, type of excipient used and tablet porosity
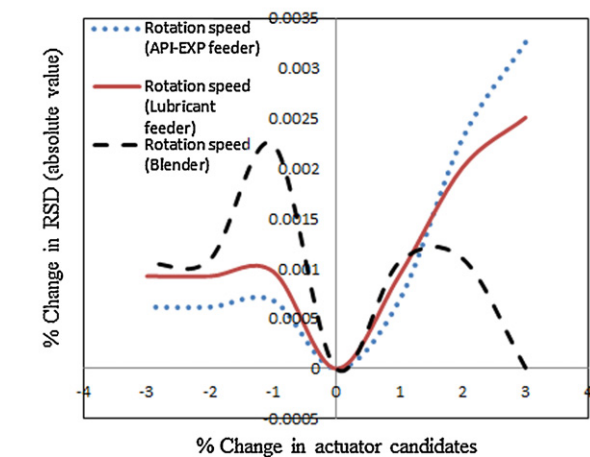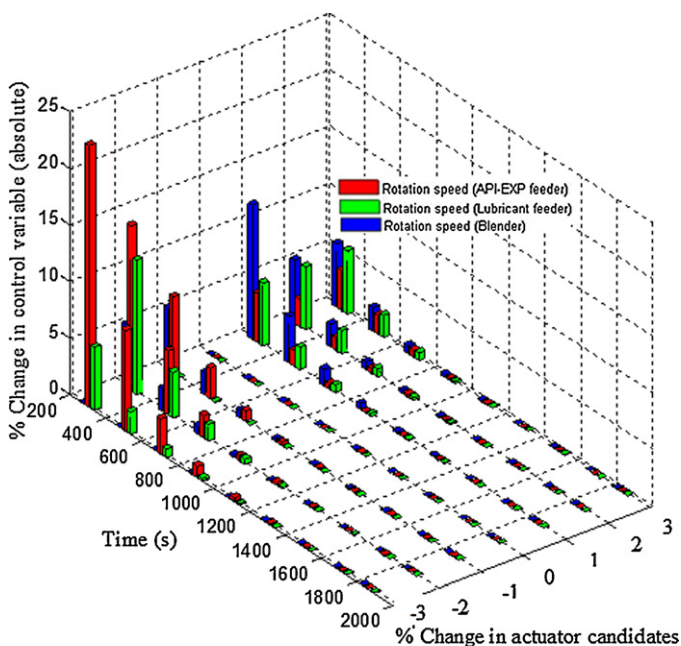
Fig. 6. Selection of actuator for RSD control: (a) 3D visualization, (b) 2D visualization.

can also affect dissolution .Therefore, an additional controller is included to adjust the hardness set point through the measurement of dissolution by a soft sensor. Table 3 consists of a list of controlled variables, controller configuration and corresponding actuators.

4.4. Measurement techniques and tools (step 6)

Within the ERC-SOPS, the measurement techniques and tools for real time measurement of the different variables involved in

the continuous tablet manufacturing pilot plant is being evaluated and combined with the proposed control system to integrate into the pilot plant, which is a subject of research and development within the center. Some of the monitoring techniques are reported in the scientific literatures (Blanco and Alcalá, 2006; Huang et al., 2002; Prats-Montalbán et al., 2012; Roggo et al., 2005; Singh et al., 2010a, 2010b; Sorokin & Gugnyak, 1973; Vanarase et al., 2010).

4.5. Controller selection (step 7)

The regulatory/basic control system (PID) has been selected for this process. The tuning control parameters are gain (K_C), reset time (K_I), and rate (K_D). As given in Table 3 there are 4 cascades, 3 single-loops and one cascade with three controllers involved in the process. Therefore, total 14 PID controllers are required and 42 controller parameters need to be tuned. For maintaining consistent API excipient ratio, a ratio controller is required. State of the art techniques have been used to improve the controller performance. Some of them are described as below:

- **Anti-windup:** An anti-windup reset algorithm is included in the model to ensure that the controller output lies within the specified upper and lower bounds. If the bounds are violated, the time derivative of the integral error is set to zero and the controller output is clipped to the bounds. Once the controller output is back in the range of the bounds, the integral error will change according to the current error.
- **Bump-less switching:** The model algorithm supports bump-less switching between different classes and modes to eliminate any undesirable disturbance into the process when changing the operation mode or the algorithm class.
- **Rate limit:** To change the value of the derivative part with certain factor, a term called rate limit has been introduced. If the value of the rate limit is 1 then it means the calculated derivative term and the applied derivative term are same while the rate limit value of less than 1 means the applied derivative term is more than the calculated value. Similarly the rate limit value of more than one means the applied derivative term is less than the calculated value.
- **Input and output bounds:** To avoid the getting of undesired controller outputs, minimum and maximum limits of the controller output have been introduced. Anti-windup algorithm will keep the controller outputs within the specified limit. Similarly, the minimum and maximum limits of the controller input have also been introduced that helps to improve the controller performance. However, the controller inputs can violate the specified limits.
- **Scaling:** Scaling factors for controller input, output and set-point have been introduced to improve the controller performance.

Table 3
Controller configuration for controlled variables and their actuators.

Critical process points	Controlled variables	Controller configuration	Intermediate actuator	Final actuator
Blender	RSD (y_{11})	Cascade	Lubricant flow rate (y_{12})	Rotation speed of lubricant feeder (u_1)
	Total flow rate (y_{21})	Cascade	API flow rate (y_{22})	Rotation speed of API feeder (u_2)
	API composition (y_3)	Single loop control	–	Rotation speed of blender (u_3)
	API Excipient ratio (y_4)	Ratio controller	–	Rotation speed of excipient feeder (u_4)
Roller compactor	Ribbon density (y_{51})	Cascade	Roller gap (y_{52})	Hydraulic pressure (u_5)
	Throughput (y_6)	Single loop control	–	Roller speed (u_6)
Milling	Granule size (y_7)	Single loop control	–	Mill rotation speed (u_7)
Tablet press	Tablet weight (y_{81})	Cascade	Pre-compression force (y_{82})	Feed volume (y_8)
	Tablet dissolution (y_{91})	Cascade	Hardness (y_{92}), Main compression force (y_{93})	Punch displacement (u_9)

4.6. Controller parameters tuning (step 8)

The controller tuning parameters (K_C: gain, K_I: reset time, K_D: rate) are tuned using the ITAE (Integral of Time Absolute Error) criteria (Seborg et al., 2004). The objective function has been minimized using the optimization routine of gPROMS and controller parameters have been identified that gives the minimum error. The first principle model as given in Appendix A has been used to perform the optimization. The objective function has been formulated as follows (n is the total number of control loops, V_i is the ith controlled variable, V_{set}^i is the set point of ith controlled variable):

$$\text{OBJ} = \sum_{i=1}^{n} \left(\int_0^t t \left| V^i - V_{set}^i \right| \ dt \right)$$

Prior to performing the optimization, all the control loops were implemented in the flowsheet model using the graphical user interface (GUI) of gPROMS as shown in Fig. 8. In gPROMS, it is possible to switch between all classes (P, PI, PID, D, PD and I) and modes (manual, automatic and cascade) using the appropriate selectors to study the controller performance in different scenario. Other than tuning controller parameters, there are other control parameters that need to be specified appropriately to achieve the better controller performance (see Appendix B). These parameters are minimum input, maximum input, minimum output, maximum output, bias, rate limit. In addition to that, it need to be determined if the control action should be direct or reverse. The tuned control parameters together with the other specifications are given in Table 4.

4.7. Proposed process control system (step 9)

4.7.1. Designed control system

The control system is systematically represented as shown in Fig. 7 for easier implementation in manufacturing plant. As highlighted (bold letter) in the figure, there are 9 variables ($y_{11}, y_{21}, y_3, y_4, y_{51}, y_6, y_7, y_{81}, y_{91}$) that need to be controlled at their predefined set points ($y_{11\_set} \ldots y_{91\_set}$). As shown in the figure (see the highlighted part), the measured total flow rate (y_{21}) is feedback to a master PID controller (PID$_{21}$) that generates the set point of API flow rate (y_{22_set}) for slave controller (PID$_{22}$). The measured API flow rate (y_{22}) is feedback to slave controller (PID$_{22}$) that generates the API feed rpm actuator (u_2) signal for the plant. Similarly, the other control loops has been designed as shown in Fig. 7.

4.7.2. Implemented control system

The designed control system (Fig. 7) has been implemented in a continuous tablet manufacturing process model implemented in gPROMS. The implemented control system is shown in Fig. 8. The controlled variables and corresponding actuators together with the Input/Output signal from each PID controller is also shown in the figure. For example, measured RSD is the input for PID$_{11}$ (master controller). Output (y_{12_set}) of PID$_{11}$ is the input of PID$_{12}$ (slave controller). The measured lubricant flow rate (y_{12}) is a second input to PID$_{12}$. The output from PID$_{12}$ is the final actuator (RPM: u_1). For each controller a set of specifications are provided as shown in Fig. B.1 (see Appendix B). The specifications of all control loops are given in Table 4.

The performance of the proposed control system is evaluated in Section 5 (step 10).

5. Results and discussion

In this section, the closed-loop performance of tablet manufacturing process has been evaluated and compared against open-loop conditions. The performance of control system for disturbance rejection and set point tracking is analyzed separately as discussed in the following sections.

5.1. Disturbance rejection

In this section the ability of the control system to reject the unknown disturbances that could be present in the tablet manufacturing process has been analyzed. The disturbances have been added to the feed streams to represent inherent feed rate variability as well as to the controlled variables directly to represent the measurement noise. The major disturbances introduced are structural sinusoidal form ($a \times \sin(t/10)$) with different amplitudes as well as random disturbances. The intensity of the structural disturbances is greater than 5%. The upper and lower control limits of the variables are also provided which are 2% more and less of set point respectively. The controller performance is considered good if it is able to maintain the controlled variables within the provided control limits.

The performance of flow rate (from blender) controller is shown in Fig. 9a. The structural disturbances in powder feed property (bulk density) as well as a measurement error at outlet flow rate from blender has been introduced. As shown in the figure in open-loop scenario the flow rate violates the control limits therefore a controller is needed to maintained the flow rates within the specified control limits irrespective of the disturbances. After introducing a cascade PID controller, the total flow rate tracks the set point and is within the control limits meaning that the controller performance is satisfactory. Similarly, the performance of the controllers implemented for RSD and API composition control are analyzed and found to be satisfactory.

The performance of the controller for ribbon density (from roller compactor) control is shown in Fig. 9b. The disturbances introduced in the blending process have been propagated to the roller compaction process. Additional disturbances to represent the unknown disturbances and measurement errors have been also introduce in the roller compaction operation. As shown in the figure, in the open-loop scenario, the ribbon density violates the control limits signifying the needs of a suitable control system. Therefore a cascade PID controller to control the ribbon density has been implemented. The implemented control system as shown in the figure is able to reject the disturbances and maintained the ribbon density within the control limit.
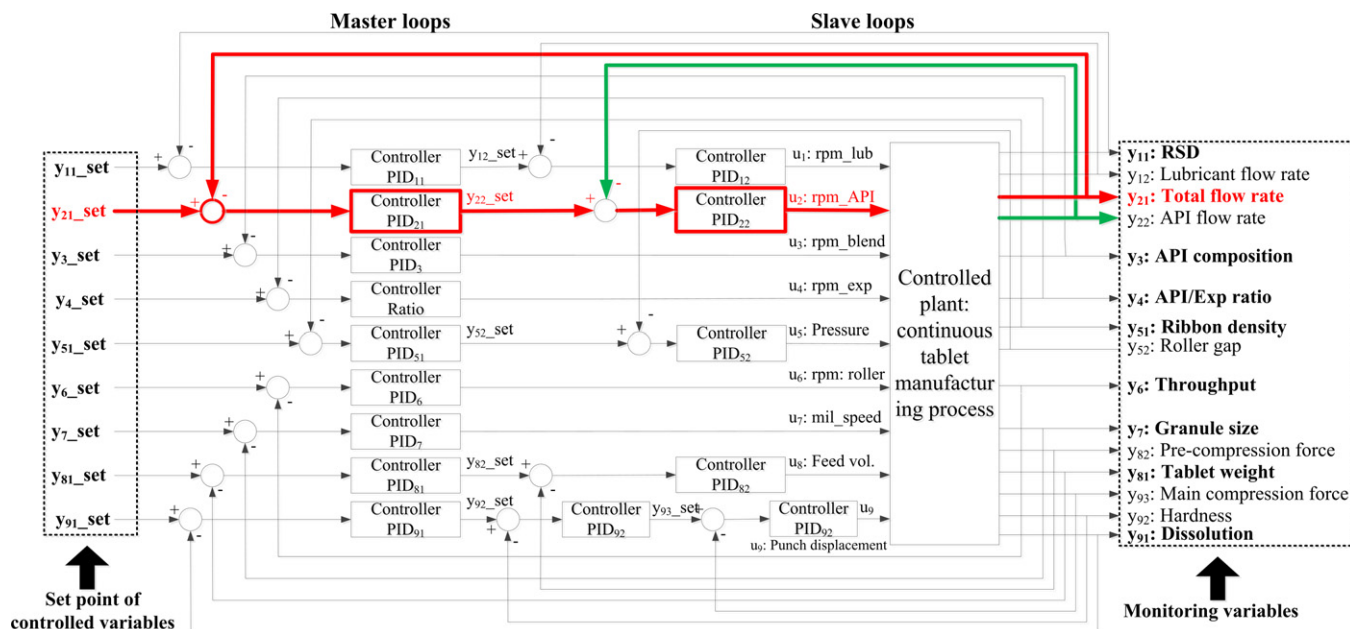
The performance of control system for controlling the throughput from roller compactor is shown in Fig. 9c. Several disturbances are affecting this control loop. For example, disturbances introduced in blending operation and in ribbon density propagates to this control loop. Addition to that, some disturbances is also introduced in throughput to accommodate the measurements error. As shown in the figure, without controller throughput violates the specified limits because of disturbances. Therefore a single-loop PID controller is implemented to reject the disturbances and to maintain the throughput at a given set point. The figure shows that the controller performance is satisfactory.

The performance of tablet weight controller is shown in Fig. 9d. As shown in the figure, in closed-loop scenario the tablet weight is consistent at pre-specified set point while in open-loop scenario the tablet weight violates the upper and lower control limits. The oscillatory response is because of structural disturbances introduced in powder feed as well as in weight measurement. Addition to that the disturbances introduced in the unit operations before the tablet press also affects the tablet weight. A cascade PID controller implemented for weight control efficiently rejects the disturbances.

The performance of the dissolution controller is shown in Fig. 10. The disturbances from the upstream affect the dissolution. The local structural dissolution measurement noise has also been added. As shown in the figure in open-loop scenario, the dissolution violates

Table 4
Controller parameters.

Control-loop	Controller	Gain (K_C)	Reset time (K_I)	Rate (K_D)	Minimum input	Maximum input	Minimum output	Max output	Bias	Rate limit	Control action
RSD	$C_{1,1}$	0.01	1	0.5	0	0.01	0	20	0	1	Direct
	$C_{1,2}$	0.01	1	0.5	0	1	0.00001	1	0	1	direct
Flow rate	$C_{2,1}$	0.8	0.001	10	15	25	0.01	10	0	1	Direct
	$C_{2,2}$	2	0.0005	0.5	9	11	0.6	0.8	0	1	Direct
API composition	C_3	0.02	0.01	0.01	0	1	0.001	6	0	1	Reverse
Ratio	C_4	–	–	–	0	1	0	1	0	–	–
Ribbon density	$C_{5,1}$	1	10	0	800	1200	1E−5	1E−2	0	1	Reverse
	$C_{5,2}$	1	10	0.1	0	1E−2	1E5	1E7	0	1	Reverse
Throughput	C_6	1	10	0	0.1	0.4	0.1	100	0	1	Direct
Granule size	C_7	1	10	0.1	1E−6	1E−4	0	1E6	0	1	Reverse
Weight	$C_{8,1}$	1	10	0	2E−4	4E−4	5	20	0	1	Direct
	$C_{8,1}$	1	10	0	14	16	2E−6	3E−6	0	1	Direct
Dissolution	$C_{9,1}$	10	0.01	0	0.89	0.95	50	160	0	1	Reverse
	$C_{9,2}$	10	0.01	1	100	140	0.001	30	0	1	Direct
	$C_{9,3}$	5	10	10	0.001	0.02	1E−7	2.3E−3	0	1	Direct

Fig. 7. Designed control system. rpm (revolution per minute): rotation speed.

the control limits while in closed-loop scenario the dissolution is within the limits. A small overshoot can be seen at initial phase of operation. The performance of dissolution control depends on the performance of three controllers implemented in cascade scheme: (1) Master controller for dissolution, (2) Slave controller for hardness, (3) Slave controller for main compression force.

5.2. Set point tracking

To analyze the ability of the controller to track the provided set point, the step changes in the set point have been made in final product quality (dissolution) and all the throughputs. There are also minor random and structural disturbances to account for unknown disturbances in the plant related to feeds and measurements. In open-loop scenario, the set points of the variables can not be tracked; therefore the open-loop responses have not been shown in this section. However, to quantify the performance of

controllers, the ITAE value of each master control loop is calculated and given in Table 5.

The closed-loop response of total flow rate at blender outlet is shown in Fig. 11. The total flow rate is controlled through a cascade control system therefore the result shown is based on the performance of two PID controllers. As shown in the figure, the total flow rate follows the given set point. However, the flow rate

Table 5
ITAE value of main control loops.

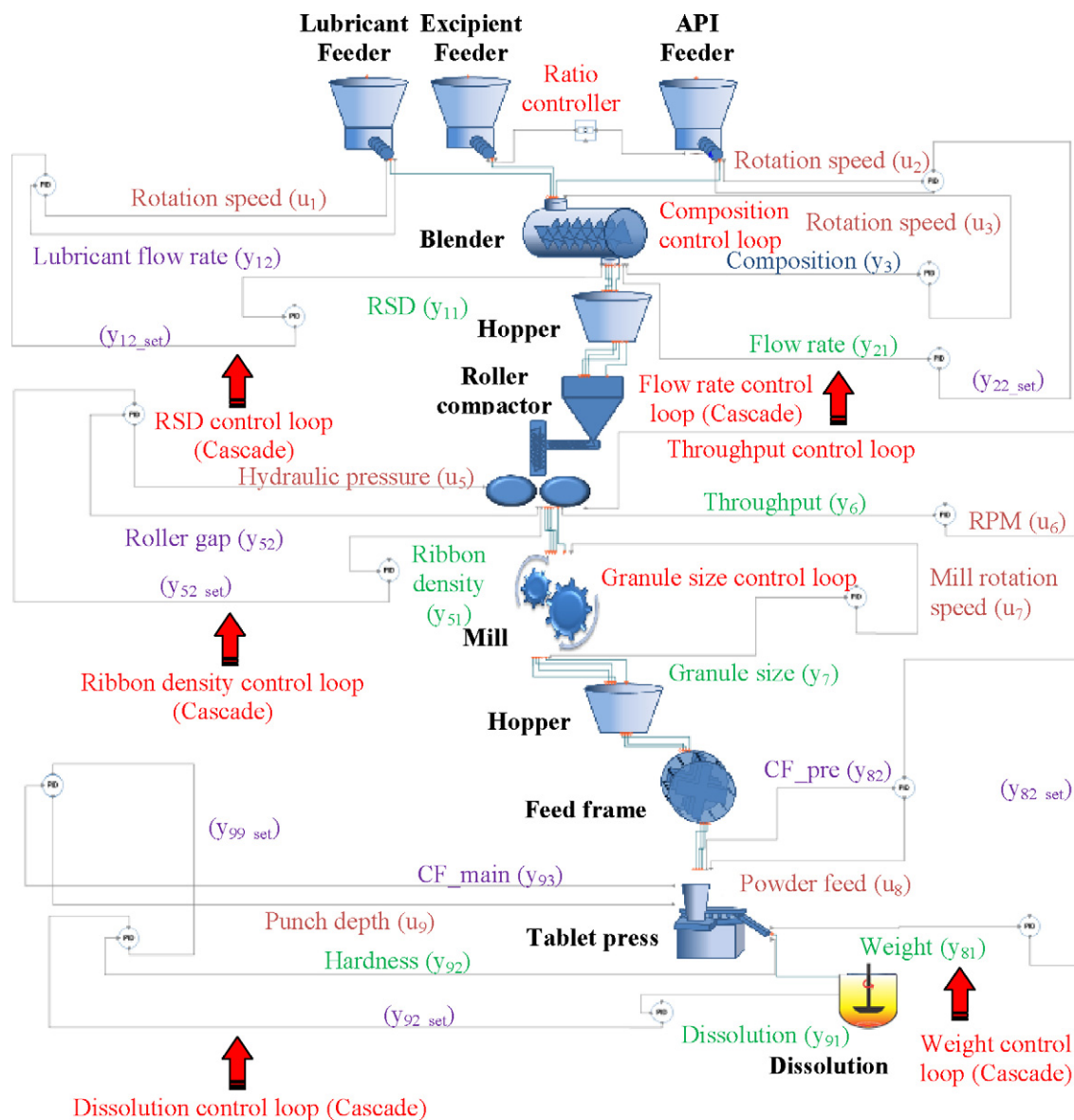| Controlled variables	ITAE
Flow rate	2.31E8
API composition	2.26E8
RSD	2.30E6
Ribbon density	8.04E5
Throughput	2.30E3
Tablet weight	2.89
Tablet dissolution	5.11

ARTICLE IN PRESS

**Fig. 8.** Closed-loop process flowsheet. CF: Compression force.

violates the control limits. The oscillatory response of this control loop may be because of large delay time involved; therefore model predictive controller for this control loop could enhance the control performance. The ITAE vale of the master control loop is found to be 2.31E8.

Fig. 12a shows the closed-loop response of API composition at blender outlet. As shown in the figure, the controller maintains the API composition at desired set-point by manipulating the rotation speed of blender. A very smooth control performance with very small oscillation and no overshoot as well as less settling time can be seen in the figure. However, the control system is sluggish and therefore the ITAE value (2.26E8) is higher.

The control loop performance of RSD, an important variable to quantify the homogeneity of the powder at blender outlet, is shown in Fig. 12b. Blender is divided in small compartments and in each compartment the powder mixing is modeled through complex PBM equation (model is given in Appendix A). The RSD is a highly correlated variable and could depends on several other operational parameters including feed rate, residence time of powder in blender, blender speed and therefore is one of the difficult controlled variables. Fig. 12b shows a satisfactory performance of RSD

control loop. The RSD settled down at given set point with reasonable settling time and small oscillation. ITAE value of this control loop is found to be 2.30E6. A very high overshoot at the beginning has been observed that could be because of the complexity of very high interactive system. The high value of ITAE value is because of this overshoot. It should be noted that RSD is controlled through a cascade control system with rotation speed of lubricant feeder as the final actuator.

The performance of controllers implemented in roller compactor is also shown in Fig. 12. The ribbon density is controlled very well at the given set point as shown in Fig. 12c. The settling time is very less meaning that the controller is very robust in this case. A very small overshoot has been observed. Ribbon density is controlled through a cascade control system with final actuator being the hydraulic pressure. Slave loop control the roller gap set point generated through master loop that controls ribbon density. The ITAE value of the master control loop is found to be 8.045E5. Change in roller gaps affects the throughput therefore to compensate that effect a second PID controller is also implemented. The step change in the set point of throughput has been made. This PID controller as shown in Fig. 12d, track the set point by manipulating the roll speed.
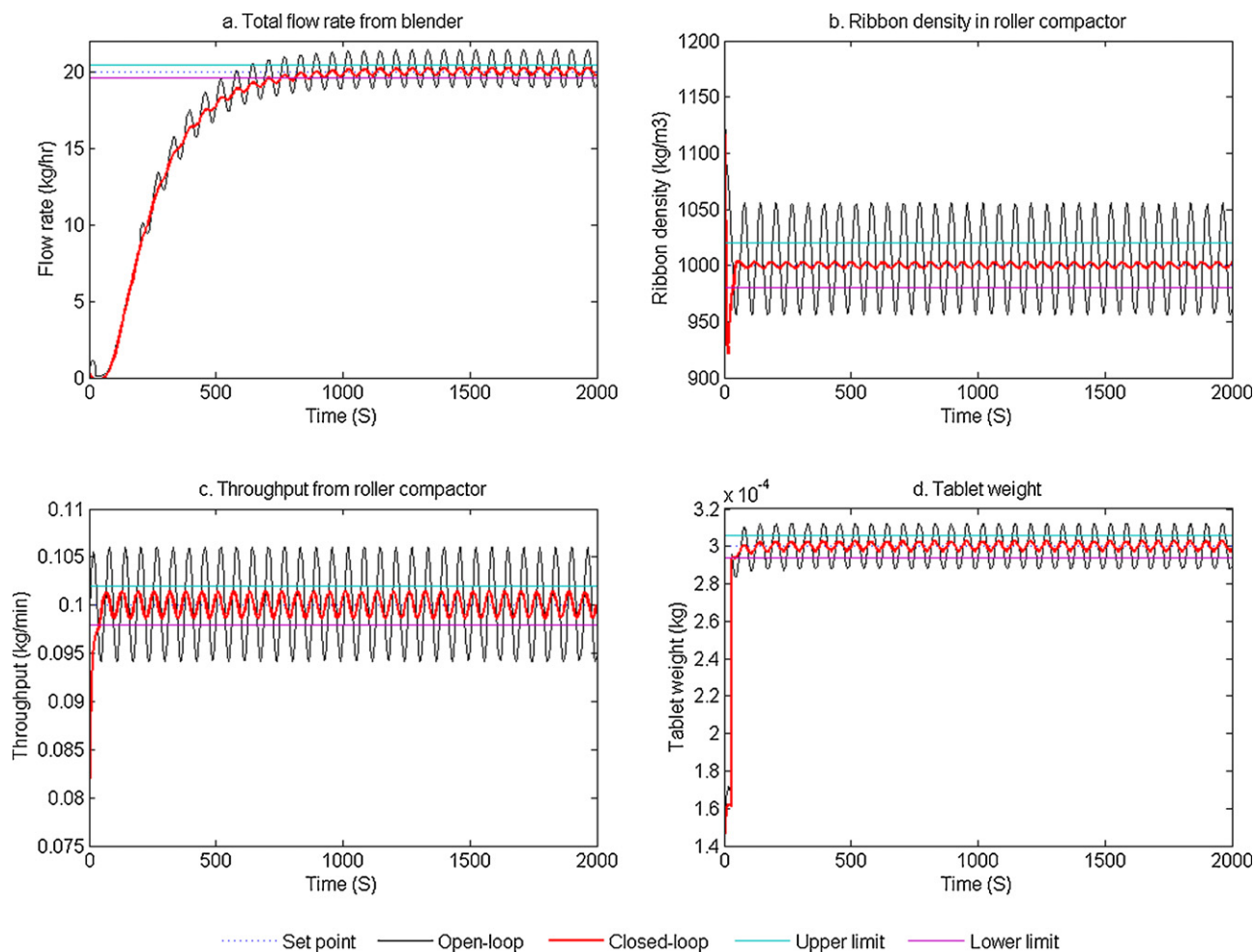
Fig. 9. Closed-loop process performance (disturbances rejection): (a) total flow rate from blender, (b) ribbon density in roller compactor, (c) throughput from roller compactor, (d) tablet weight.

The performance of this controller is good with no overshoot and oscillation. The ITAE value for this control loop is found to be 2.30E3.

The performance of the control loop for tablet weight control is shown in Fig. 13a. As shown in the figure, the tablet weight is maintained at the given set point. The tablet weight is controlled through a cascade control system. The master loop provides the set point of pre-compression pressure while the slave loop track the pre-compression pressure set point by manipulating the powder
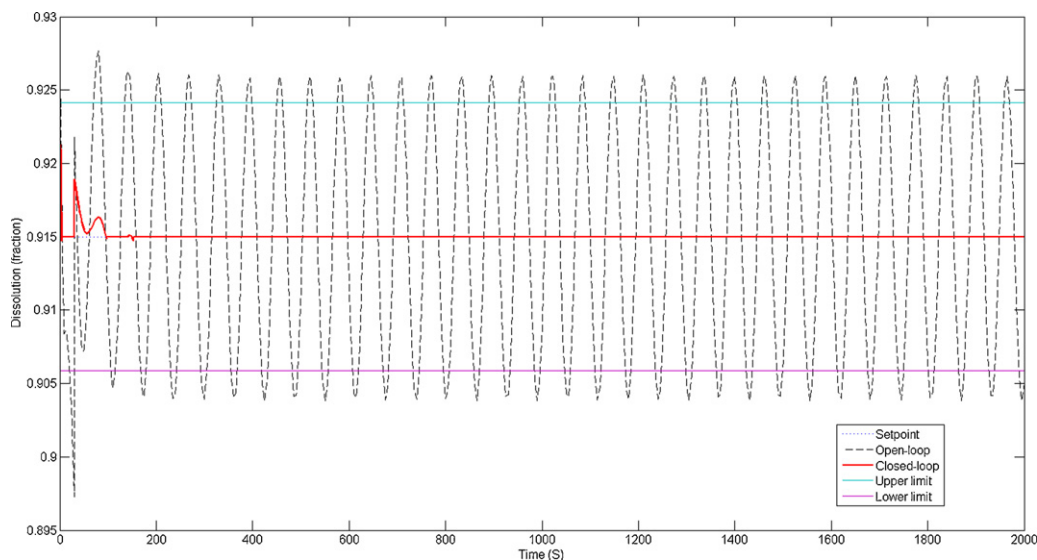
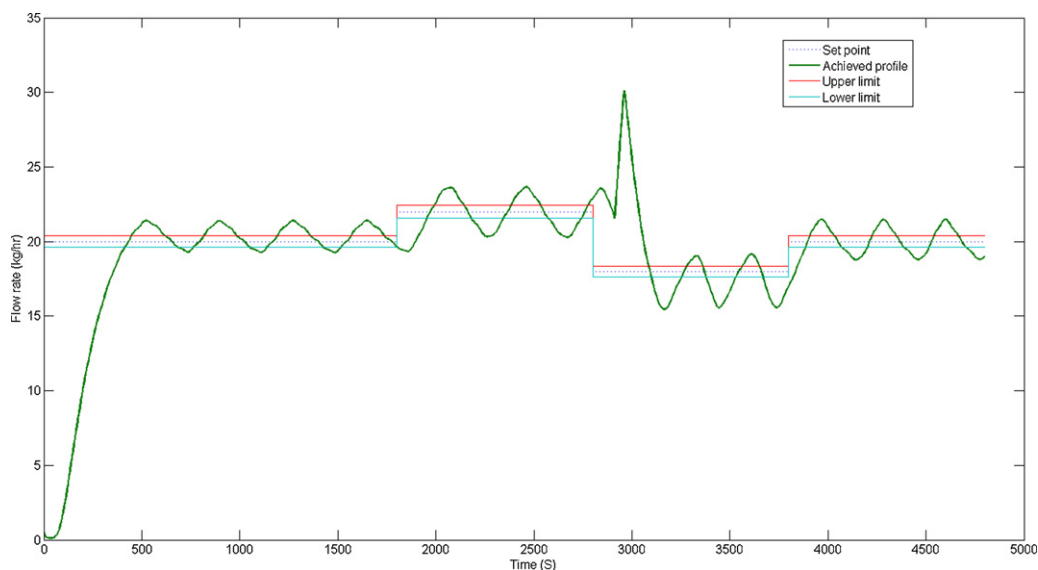**Fig. 10.** Control of dissolution (disturbances rejection).

Fig. 11. Control of total flow rate (set point tracking).

feed rate. The ITAE value for master loop is found to be 2.89 that show a good set point tracking.

In order to control the dissolution, three controllers have been implemented. The step change in the set point of dissolution has been made as shown in Fig. 14. The master controller tracks the set point of dissolution and generates the hardness set point as shown in Fig. 13b. As shown in Fig. 14, a small overshoot has been observed at the starting point and except that the controller performance is satisfactory for dissolution control. The ITAE value of the master control loop is found to be 5.11. Hardness is control through a slave cascade controller. The performance of the hardness control loop is shown in Fig. 13b. The set point for this control loop is generated by a master controller. As shown in the figure, during startup phase the set point obtained by master controller is too high that

has not been tracked by the slave controller. However, after this point, the performance of the controller is satisfactory. The hardness controller also has a slave controller for controlling the main compression pressure by manipulating the punch displacement.

The performance of the proposed control system (shown in Fig. 7) is found to be satisfactory, therefore this control system can be considered for implementation in the plant (step 11). The advanced techniques (discussed in Section 4.5) that have been integrated with the proposed control system enhanced the performance of the controllers. The proposed control system is being implemented in a pilot plant described in Section 3.1 (step 12). The integration of the pilot plant with sensors, control softwares and hardware is discussed in this section. The process variables are measured online using the appropriate sensors (e.g. NIR for composition or RSD
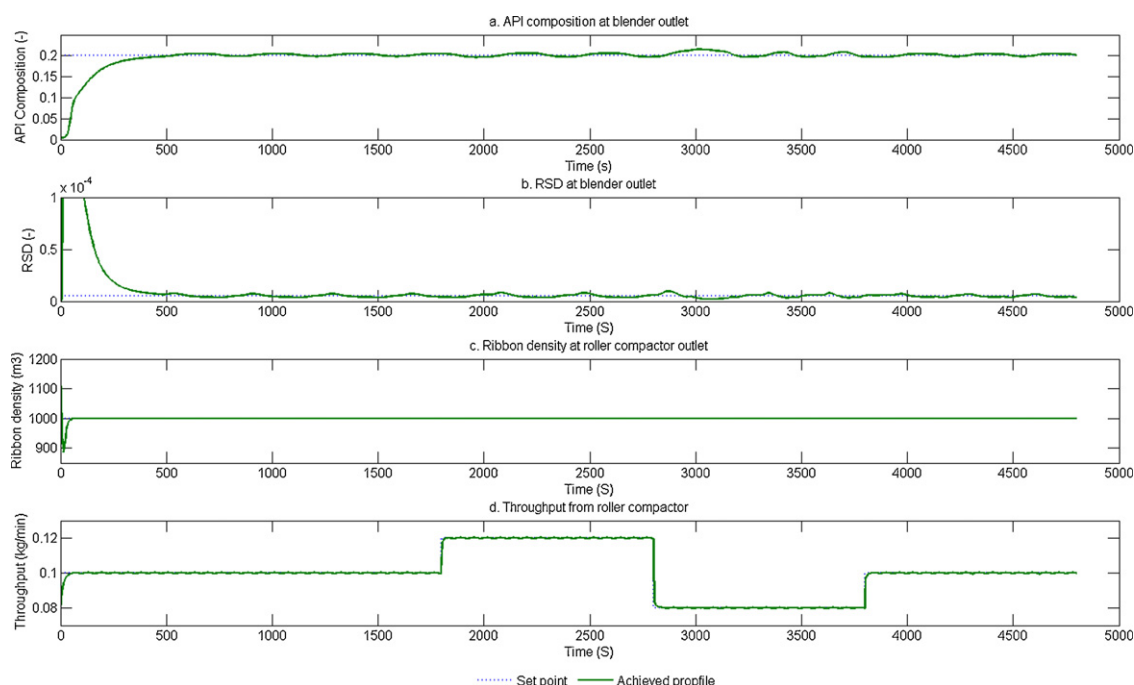

Fig. 12. Closed-loop performance (set point tracking): (a) API Composition, (b) RSD, (c) ribbon density, (d) throughput of roller compactor.
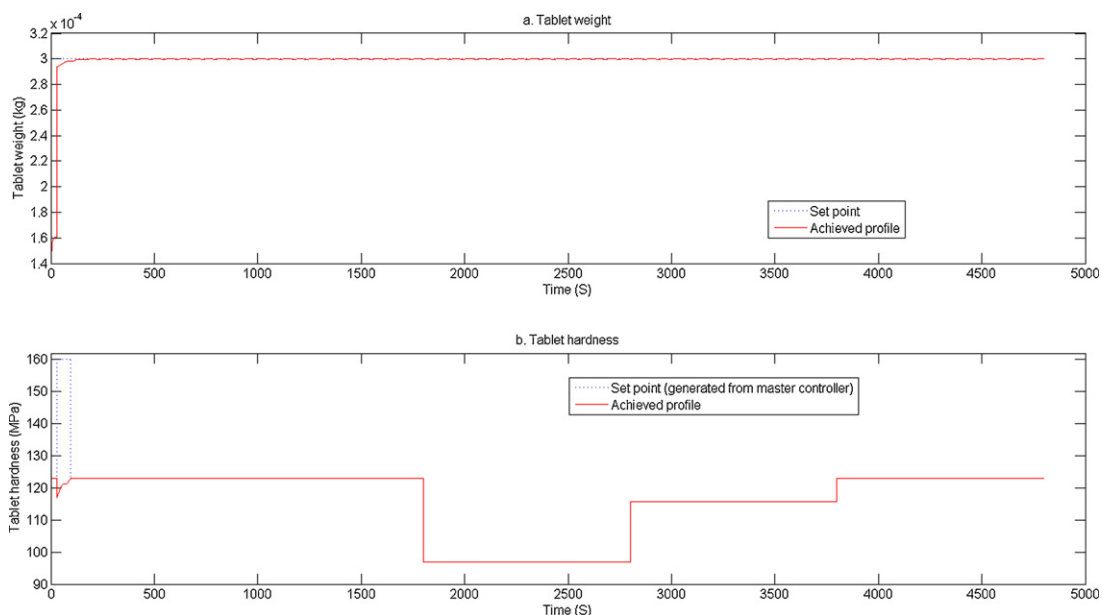
ARTICLE IN PRESS

Fig. 13. Closed-loop performance (set point tracking): (a) tablet weight and (b) tablet hardness.
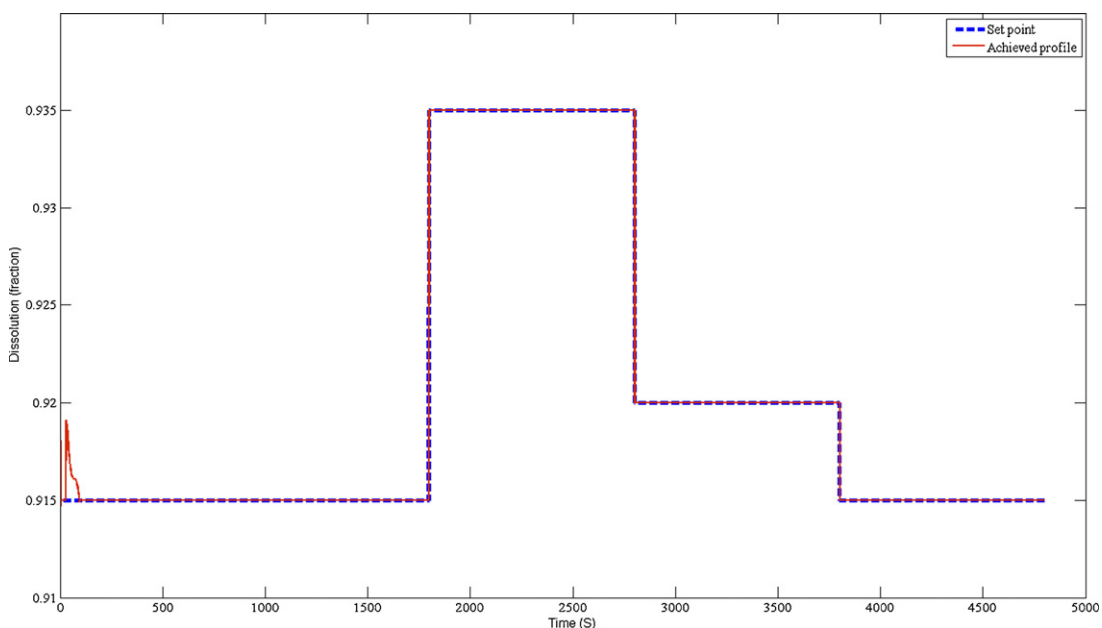

Fig. 14. Control of tablet dissolution (set point tracking).

measurements). The sensor output is connected with a computer in which the monitoring and control softwares are installed (e.g. synTQ (synchronized Total Quality, Optimal Industrial Automation), SIMCA QP (Umetrics)). PAT Data Management tool synTQ uses SIMCA QP to convert the measured spectrum into a meaningful signal (e.g. composition). The signal conversion is needed only for spectroscopic sensors and for other sensors, the signal can be directly sent to the control hardware. The controllers (e.g. PID) and the corresponding control parameters are provided through the user interface to calculate the actuators. The signals are then sent by synTQ to the control hardware (deltaV, Emerson) using the OPC communication protocol. DeltaV communicate with the plant through digital communication cards (e.g. DeviceNet or Profibus) and manipulate the actuators.

6. Conclusions

To produce the pharmaceutical product of consistent predefined end product quality is of crucial importance. A well-designed control system is essential to obtain the desired product quality consistently. In this work we designed a control system combining feedback and cascade strategies for a continuous tablet manufacturing process. The manufacturing process uses a roller compactor as a means of dry granulation. The control system has been implemented in a first principle model simulated in gPROMS. The first principle model has also been reported. An effective controller parameter tuning strategy involving ITAE methods coupled with optimization routine of gPROMS has also proposed. The state of the art techniques (e.g. anti-windup) have been employed to improve

the performance of the control system. The ability of the control system for disturbances rejection and set point tracking has been analyzed. The performance of the control system is found to be satisfactory and able to reject the unknown disturbances as well as able to track the set points. The response of the controller to track the set point of total flow rate from blender is found to be oscillatory and less satisfactory that could be improved using advanced model predictive controller (MPC). The proposed control system has a wide range of applications in pharmaceutical industry to run the plant safely, reduce the number of rejected batches, to achieve the predefined end product quality consistently and to satisfy the regulatory requirements. Future work includes the development of more advanced control system (e.g. MPC) and its implementation in our continuous tablet manufacturing pilot plant through the commercially available hardware (e.g. Delta V) and control interface (e.g. OPC).

Acknowledgements

Appendix A. Continuous tablet manufacturing

A.1. Feeder

The parameters of the feeder unit operation model consist of the process gain parameter (k_g^f), the time constant (τ^f), and the time delay factor (θ_d^f) (Eq. (A.1)). The optimum parameter values were obtained through minimization of the least-squares error of the observed versus predicted flowrate values. As described in Section 2, the inlet bulk density and mean particle size are assumed to be constant and are input specifications of the material being fed to the model (Boukouvala et al., in press).

$$\tau^f \frac{dm_{out}(t)}{dt} + m_{out}(t) = k_g^f \omega^f$$

$$\theta_d^f \frac{\partial m_{out}^{delayed}(t,z)}{\partial t} = -\frac{\partial m_{out}^{delayed}(t,z)}{\partial z} \quad \text{with I.C. } m_{out}^{delayed}(t, z = 0) = m_{out}(t) \tag{A.1}$$

$$\rho_{bulk\_in}(t) = \rho_{bulk\_out}(t)$$

$$d_{50\_in}(t) = d_{50\_out}(t)$$

where ω^f is the feeder screw rotation rate, z is the time delay domain, and $m_{out}^{delayed}$ is the actual output feed rate of the material based on the experimentally observed time delay θ_d^f.

A.2. Blender

A.2.1. Process model

A multi-dimensional population balance model is constructed to model blending processes that accounts for n solid components and two external coordinates (axial and transverse directions in the blender) and one internal coordinate (size distribution due to segregation). The detail of the blending process model is previously reported (Sen and Ramachandran, in press; Sen et al., 2012). The equation is shown below:

$$\frac{\partial F(n, z_1, z_z, r, t)}{\partial t} + \frac{\partial}{\partial z_1}\left[F(n, z_1, z_2, r, t)\frac{dz_1}{dt}\right]$$

$$+ \frac{\partial}{\partial z_2}\left[F(n, z_1, z_2, r, t)\frac{dz_2}{dt}\right] + \frac{\partial}{\partial r}\left[F(n, z_1, z_2, r, t)\frac{dr}{dt}\right]$$

$$= \Re_{formation}(n, z_1, z_2, r, t) - \Re_{depletion}(n, z_1, z_2, r, t) \tag{B.1}$$

In Eq. (B.1), the number density function $F(n, z_1, z_2, r, t)$ represents the total number of moles of particles with property r at position $z = (z_1, z_2)$ and time t. In addition, z_1 is the spatial coordinate in the axial direction, z_2 is the spatial coordinate in the radial direction, r is the internal coordinate that depicts particle size and z_2 to indicate presence of two components (Active Pharmaceutical Ingredient and excipient). Hence dz_1/dt and dz_2/dt represent the axial and radial velocity respectively.

$$\sum_{z_1} m_{in}^i(n = 1, z_1, z_2 = 0, t) = m_{in}^i(t) \quad for \ i = 1, .., n$$

$$m_{out}^i(t) = \sum_{z_1} m^i(n = 1, z_1, z_2 = L, t) \quad for \ i = 1, .., n$$

$$\rho_{bulk\_out}(t) = \sum_i^n C(n = i, z_1, z_2 = L, t)\rho_{bulk\_in}^i \tag{B.2}$$

$$d_{50\_out}(t) = \sum_i^n C(n = i, z_1, z_2 = L, t)d_{50\_in}^i$$

$$RSD(t) = \frac{SD(n = \text{“API”}, z_1, z_2 = L, t)}{mean(n = \text{“API”}, z_1, z_2 = L, t)}$$

The group of Eq. (B.2) is included in the mixing model for the calculation of the inlet mass flow rates of each material, the outlet bulk density, mean particle size and RSD, which are passed on the next unit operation. These equations are necessary for the connection of the population balance equation with preceding and subsequent unit operations.

A.3. Controller model

A.3.1. Total flow rate from blender (cascade PID controller)

The deviation from the set point of total flow rate is calculated:

$$error_{m_{out}} = m_{out\_set} - m_{out}$$

The set point for the slave controller (for API flow rate) is calculated on the basis of the deviation from the set point of total flow rate, using a PID control law:

$$F_{API\_set} = K_C^{m_{out}} error_{m_{out}} + \frac{1}{K_I^{m_{out}}} \int_0^t error_{m_{out}} \ dt + K_D^{m_{out}} \frac{d(error_{m_{out}})}{dt}$$

The deviation from the set point of the API flow rate is calculated as follows:

$$error_{F_{API}} = F_{API\_set} - F_{API}$$

The final actuator setting (RPM of API feeder) is calculated on the basis of the deviation from the set point, using a PID control law:

$$rpm_{API} = K_C^{F_{API}} error_{F_{API}} + \frac{1}{K_I^{F_{API}}} \int_0^t error_{F_{API}} \ dt + K_D^{F_{API}} \frac{d(error_{F_{API}})}{dt}$$

A.3.2. RSD at blender outlet (cascade PID controller)

The deviation from the set point of RSD is calculated:

$$error_{RSD} = RSD_{set} - RSD$$

The set point for the slave controller (for lubricant flow rate) is calculated on the basis of the deviation from the set point of RSD, using a PID control law:

$$F_{\text{Lub\_set}} = K_C^{\text{RSD}} \text{error}_{\text{RSD}} + \frac{1}{K_I^{\text{RSD}}} \int_0^t \text{error}_{\text{RSD}} \ dt + K_D^{\text{RSD}} \frac{d(\text{error}_{\text{RSD}})}{dt}$$

Design parameters such as roll radius R^{rol}, roll width W^{rol}, compact surface area A^{rol}, effective angle of friction δ, inlet angle θ_{in} and nip angle α need to be specified based on the geometry of the equipment and the material properties of the powder mixture. The dynamics of the process in the case of step changes in the pressure, rotation speed and feed speed are captured by the final three first order differential equations.

$$\frac{d}{dt}\left(\frac{h_0(t)}{R^{rol}}\right) = \frac{\omega^{rc}\left[\rho_{\text{bulk\_in}}(t)\cos\theta_{\text{in}}(1 + h_0(t)/R^{rol} - \cos\theta_{\text{in}})(u_{\text{in}}(t)/\omega^{rc}(t)R^{rol}) - \rho_{\text{out}}^{\text{rib}}(t)(h_0(t)/R^{rol})\right]}{\int_0^{\theta_{in}} \rho(\theta)\cos(\theta) \ d\theta}$$

$$P_h^{rc}(t) = \frac{W^{rol}}{A^{rol}} \frac{\sigma_{\text{out}}(t)R^{rol}}{1 + \sin\delta} \int_0^a \left[\frac{h_0(t)/R^{rol}}{(1 + h_0(t)/R^{rol} - \cos\theta)\cos\theta}\right]^{K^{rc}} \cos\theta \ d\theta$$

$$\sigma_{\text{out}}(t) = C_1^{rc}(\rho_{\text{out}}^{\text{rib}}(t))K^{rc} \qquad\qquad (C.1)$$

$$\tau_P^{rc} \frac{dP_h(t)}{dt} + P_h(t) = P_{sp}^{rc}$$

$$\tau_{rc}^{\omega} \frac{d\omega^{rc}(t)}{dt} + \omega^{rc}(t) = \omega_{sp}^{rc}$$

$$\tau_u^{rc} \frac{du^{rc}(t)}{dt} + u^{rc}(t) = u_{sp}^{rc}$$

The deviation from the set point of the Lubricant flow rate is calculated as follows:

$$\text{error}_{F_{\text{Lub}}} = F_{\text{Lub\_set}} - F_{\text{Lub}}$$

The final actuator setting is calculated on the basis of the deviation from the set point, using a PID control law:

$$\text{rpm}_{\text{Lub}} = K_C^{F_{\text{Lub}}} \text{error}_{F_{\text{Lub}}} + \frac{1}{K_I^{F_{\text{API}}}} \int_0^t \text{error}_{F_{\text{API}}} \ dt + K_D^{F_{\text{API}}} \frac{d(\text{error}_{F_{\text{API}}})}{dt}$$

A.3.3. API composition (PID controller)

The deviation from the set point of API composition is calculated:

$$\text{error}_{C_{\text{API}}} = C_{\text{API\_set}} - C_{\text{API}}$$

The actuator setting is calculated on the basis of the deviation from the set point, using a PID control law:

$$\text{rpm}_{\text{blender}} = K_C^{C_{\text{API}}} \text{error}_{C_{\text{API}}} + \frac{1}{K_I^{C_{\text{API}}}} \int_0^t \text{error}_{C_{\text{API}}} \ dt + K_D^{C_{\text{API}}} \frac{d(\text{error}_{C_{\text{API}}})}{dt}$$

A.4. Roller compaction

A.4.1. Process model

The model introduced in (Hsu et al., 2010a,b) is adapted in order to relate the input powder bulk density ($\rho_{\text{bulk\_in}}$) of the powder and process parameters such as compression pressure (P_h^{rc}), rotating roll speed (ω^{rc}) and inlet powder feed speed (m_{in}) to average density ($\rho_{\text{bulk\_out}}^{\text{rib}}$) and thickness ($h_0$) of the produced ribbon. The roller compactor is divided into two regions, the slip region—within which the powder is assumed to flow between the rolls, and the nip region—inside which the powder is compressed to form ribbons. The first equation is the material balance of the powder entering the nip region which is exiting in forms of ribbons. An empirical correlation is used between applied ribbon stress and density, using the values of the parameters K^{rc} and C_1^{rc} in the original publication.

A.5. Controller model

A.5.1. Ribbon density (cascade PID controller)

The deviation from the set point of ribbon density is calculated:

$$\text{error}_\rho = \rho_{\text{out\_set}}^{\text{rib}} - \rho_{\text{out\_set}}^{\text{rib}}$$

The set point for the slave controller (for roller gap) is calculated on the basis of the deviation from the set point of ribbon density, using a PID control law:

$$h_{0\_\text{set}} = K_C^{\rho} \text{error}_\rho + \frac{1}{K_I^{\rho}} \int_0^t \text{error}_\rho \ dt + K_D^{\rho} \frac{d(\text{error}_\rho)}{dt}$$

The deviation from the set point of the roller gap is calculated as follows:

$$\text{error}_{h_0} = h_{0\_\text{set}} - h_0$$

The final actuator setting (hydraulic pressure) is calculated on the basis of the deviation from the set point, using a PID control law:

$$P_h^{rc} = K_C^{h_0} \text{error}_{h_0} + \frac{1}{K_I^{h_0}} \int_0^t \text{error}_{h0} \ dt + K_D^{h_0} \frac{d(\text{error}_{h_0})}{dt}$$

A.5.2. Throughput (PID controller)

The deviation from the set point of throughput is calculated:

$$\text{error}_{Th} = Th_{\text{set}} - Th$$

The actuator setting is calculated on the basis of the deviation from the set point, using a PID control law:

$$\omega^{rc} = K_C^{Th} \text{error}_{Th} + \frac{1}{K_I^{Th}} \int_0^t \text{error}_{Th} \ dt + K_D^{Th} \frac{d(\text{error}_{Th})}{dt}$$

A.6. Milling

A.6.1. Process model

The population balance model is characterized by the internal coordinates API volume (s_1), excipient volume (s_2) and gas volume (g) (Boukouvala et al., in press). (see Eq. (D.1)):

$$\frac{\partial}{\partial T}f(s_1, s_2, g, t) = \Re_{\text{break}}(s_1, s_2, g, t)$$

$$\Re_{\text{break}}(s_1, s_2, g, t) = \Re_{\text{break}}^{\text{formation}} - \Re_{\text{break}}^{\text{depletion}}$$

$$\Re_{\text{break}}^{\text{formation}} = \int_{s_1}^{\infty} \int_{s_2}^{\infty} \int_{g}^{\infty} k_{\text{break}}(s_1', s_2', g')b(s_1, s_2, g, s_1', s_2', g') \times F(s_1', s_2', g', t)\ ds_1'\ ds_2'\ dg'$$

$$\Re_{\text{break}}^{\text{depletion}} = k_{\text{break}}(s_1, s_2, g)F(s_1, s_2, g, t)$$

(D.1)

Similarly to the mixing model, density function $F(s_1, s_2, g, t)$ represents the number of moles of particles of API, excipient and gas in time. Here, $\Re_{\text{break}}$ is the breakage rate, which is described by the difference between the rate of formation of new daughter particles and the rate of depletion of the original particle. In Eq. (D.1), the breakage rate is described by the breakage function (b) and the breakage kernel (k_{break}). As an initial condition, the mean particle size of the material that enters the mill is set to a really large value, resembling the size of broken ribbons.

The breakage kernel used in this study was a modified kernel based on the work by Matsoukas et al. (2009), where k_{break} has a size and composition (c_1, c_2) dependency, where different weights are assigned to the different components in order to introduce composition asymmetry in the model. The current kernel in the literature is symmetrical and as a result deviations in the API composition from the desired value cannot be observed. The outputs of the PBM are particle size (d_{50}), bulk density ($\rho_{\text{bulk\_out}}$) and API composition (C_{API}), which are defined as follows:

$$d_{50}(t) = \left[\frac{6(s_1(t) + s_2(t) + g(t))}{\pi}\right]^{1/3}$$

$$\rho_{\text{bulk\_out}}(t) = \frac{\text{Mass of solid}(t)}{\text{Total Volume}(t)}$$

(D.2)

$$C_{\text{API}}(t) = \frac{\sum(F(t)s_1(t))/(s_1(t) + s_2(t))}{\sum F(t)}$$

Note that in this model the evolution of the average particle diameter is tracked for all particle size ranges (i.e., fines, product and oversized particles).

A.6.2. Controller model

A.6.2.1. Granule size (PID controller).
The deviation from the set point of granule is calculated:

$$\text{error}_d = d_{50\_\text{set}} - d_{50}$$

The actuator setting (mill speed) is calculated on the basis of the deviation from the set point, using a PID control law:

$$\text{mill}_{\text{speed}} = K_C^d \text{error}_d + \frac{1}{K_I^d}\int_0^t \text{error}_d\ dt + K_D^d \frac{d(\text{error}_d)}{dt}$$

A.7. Hoppers

A mass balance on the hopper system will be of the following form (Boukouvala et al., in press) (Eq. (E.1)):

$$\frac{dm}{dt} = m_{\text{in}} - m_{\text{out}}$$

(E.1)

where $\dot{m}$ the mass holdup inside the hopper. Assuming constant bulk density throughout the hopper the height of the material inside the hopper can be correlated to the mass holdup through (Eq. (E.2)):

$$\dot{m}(t) = H^{\text{hop}}(t)A^{\text{hop}}\rho_{\text{bulk}}(t)$$

(E.2)

The area of the conical hopper is not constant and it is assumed to be a linear function of the height. This correlation can be easily found from measuring the actual dimensions of the hopper. The propagation of individual component concentrations and RSD are captured taking into account the time delay caused by the mean residence time of the material inside the hopper (Eq. (E.3)).

$$\theta_{rt}\frac{\partial C_{\text{out}}^i(t,z)}{\partial t} = \frac{\partial C_{\text{out}}^i(t,z)}{\partial z} \text{ with I.C. } C_{\text{out}}^i(t, z = 0) = C_{\text{in}}^i(t), \quad \text{for } i = 1, \dots, n$$

$$\theta_{rt}\frac{\partial \text{RSD}_{\text{out}}(t,z)}{\partial t} = \frac{\partial \text{RSD}_{\text{out}}(t,z)}{\partial z} \text{ with I.C. } \text{RSD}_{\text{out}}(t, z = 0) = \text{RSD}_{\text{in}}(t)$$

(E.3)

where H^{hop} is the height, A^{hop} is the area of the hopper, ρ_{bulk} is the bulk density and θ_{rt} the mean residence time of the material inside the hopper. In other words, since it is assumed that all the material entering the hopper flows out at a constant flowrate, it is safe to deduce that the material is no further mixed and according to its mean residence time all properties of the blend will propagate at the output of the hopper accordingly.

A.8. Tablet Press

A.8.1. Process model

The model of tablet pressing process is adapted from Singh et al. (2010a). The base area of a tablet is calculated as follows, assuming that the tablet has a cylindrical shape:

$$A = \frac{3.14d^2}{4}$$

The volume of a tablet is calculated as follows:

$$V = AL$$

The pre-compression volume is given by:

$$V_{\text{pre}} = AL_{\text{pre}}$$

A noise term is assumed to take into account the variation in porosity, and is implemented as given below:

$$n\_t_\varepsilon = A \times \sin(t/10)$$

The porosity of feed with added noise is then obtained as:

$$\varepsilon = \varepsilon_0 + n\_t_\varepsilon$$

A noise term is assumed to show the variation in feed volume, as given below:

$$n\_t_\varepsilon = A_1 \times \sin(t/10)$$

The feed volume with added noise is then:

$$V_0 = V_m + n\_t_F$$

The weight of a tablet is calculated:

$$M = (1 - \varepsilon)V_0\rho$$

The height of the powder in the die is calculated as follows:

$$L_{\text{depth}} = \frac{V_0}{A}$$

The displacement of the upper punch in the compression process is calculated as follows.

$$L_{\text{punch\_displ}} = L_{\text{depth}} - L$$

The dwell time is calculated as follows:

$$t_{\text{dwell}} = \frac{L_{\text{punch\_displ}}}{u}$$

All the expressions for compression pressure are derived from the Kawakita compression equation (Kawakita and Ludde, 1971). An intermediate term used for calculation of pre-compression pressure is first computed:

$$\lambda_{\text{pre}} = b(V_0(\varepsilon - 1) + V_{\text{pre}})$$

The pre-compression pressure is given by:

$$C\_P_{\text{pre}} = \frac{b(V_0 - V_{\text{pre}})}{\lambda_{\text{pre}}}$$

The pre-compression force is given by:

$$C\_F_{\text{pre}} = 10^6 C\_P_{\text{pre}}A$$

The right hand side of the above equation is multiplied by 10^6 to adjust the unit of force.

The porosity of the powder after the pre-compression is then calculated:

$$\varepsilon_{\text{main}} = 1 - \frac{(1 - \varepsilon)V_0}{V_{\text{pre}}}$$

The intermediate term used for calculation of the main compression pressure is given by:

$$\lambda_{\text{main}} = b(V_{\text{pre}}(\varepsilon_{\text{main}} - 1) + V)$$

The main compression pressure is given by:

$$C\_P_{\text{main}} = \frac{b(V_{\text{pre}} - V)}{\lambda_{\text{main}}}$$

The main compression force is obtained as:

$$C\_F_{\text{main}} = 10^6 C\_P_{\text{main}}A$$

The solid volume of powder is given by:

$$V_s = (1 - \varepsilon)V_0$$

The relative density is defined as follows:

$$\rho_r = \frac{V_s}{V}$$

An intermediate term used for hardness calculation is then introduced:

$$\lambda_H = \ln\left(\frac{1 - \rho_r}{1 - \rho_{rc}}\right)$$

The hardness of a tablet is calculated as (Kuentz and Leuenberger, 2000):

$$H = H_{\text{max}}(1 - \exp(\rho_r - \rho_{r_{cr}} + \lambda_H))$$

The tablet production rate is given by:

$$\frac{d(N_{Tab})}{dt} = r_{Tab}$$

A.9. Controller model

A.9.1. Tablet weight (cascade PID controller)
The deviation from the set point of tablet weight is calculated:

$$\text{error}_M = M_{\text{set}} - M$$

The set point for the slave controller (for pre-compression pressure) is calculated on the basis of the deviation from the set point of tablet weight, using a PID control law:

$$C\_P_{\text{pre\_set}} = K_C^M \text{error}_M + \frac{1}{K_I^M}\int_0^t \text{error}_M \, dt + K_D^M \frac{d(\text{error}_M)}{dt}$$

The deviation from the set point of the pre-compression pressure is calculated as follows:

$$\text{error}_{C\_P_{\text{pre}}} = C\_P_{\text{pre\_set}} - C\_P_{\text{pre}}$$

The final actuator setting (feed volume) is calculated on the basis of the deviation from the set point, using a PID control law:

$$L_{\text{punch\_displ}} = K_C^{\text{main}} \text{error}_{C\_P_{\text{main}}} + \frac{1}{K_I^{\text{main}}}\int_0^t \text{error}_{C\_P_{\text{main}}} \, dt + K_D^{\text{main}} \frac{d(\text{error}_{C\_P_{\text{main}}})}{dt}$$

A.9.2. Tablet hardness (cascade PID controller)
The deviation from the set point of tablet hardness is calculated:

$$\text{error}_H = H_{\text{set}} - H$$

H_{set} is calculated in Section A.10.2 based on error in dissolution. The set point for the slave controller (for main-compression pressure) is calculated on the basis of the deviation from the set point of tablet hardness, using a PID control law: $C\_P_{\text{main\_set}} = K_C^H \text{error}_H + \frac{1}{K_I^H}\int_0^t \text{error}_H \, dt + K_D^H \frac{d(\text{error}_H)}{dt}$

The deviation from the set point of the main-compression pressure is calculated as follows:

$$\text{error}_{C\_P_{\text{main}}} = C\_P_{\text{main\_set}} - C\_P_{\text{main}}$$

The final actuator setting (punch displacement) is calculated on the basis of the deviation from the set point, using a PID control law:

$$V_m = K_C^{\text{pre}} \text{error}_{C\_P_{\text{pre}}} + \frac{1}{K_I^{\text{pre}}}\int_0^t \text{error}_{C\_P_{\text{pre}}} \, dt + K_D^{\text{pre}} \frac{d(\text{error}_{C\_P_{\text{pre}}})}{dt}$$

A.10. Dissolution model

A.10.1. Process model
Dissolution of each component i at the solid–fluid interface is modeled as a first order rate process and its subsequent diffusion in the surrounding fluid phase is modeled using Fick's second law with a variable diffusion coefficient. The following set of partial differential equations governs the dissolution process (Kimber et al., 2011):

$$\frac{\partial C_i}{\partial t} = -\nabla \cdot (-D_i \nabla C_i) + S_i \tag{G.1}$$

$$S_i(x) = \begin{cases} k_i(C_i^{sat} - C_i(x)), & \forall x : \phi_i(x) > 0 \\ 0, & \text{otherwise} \end{cases} \tag{G.2}$$

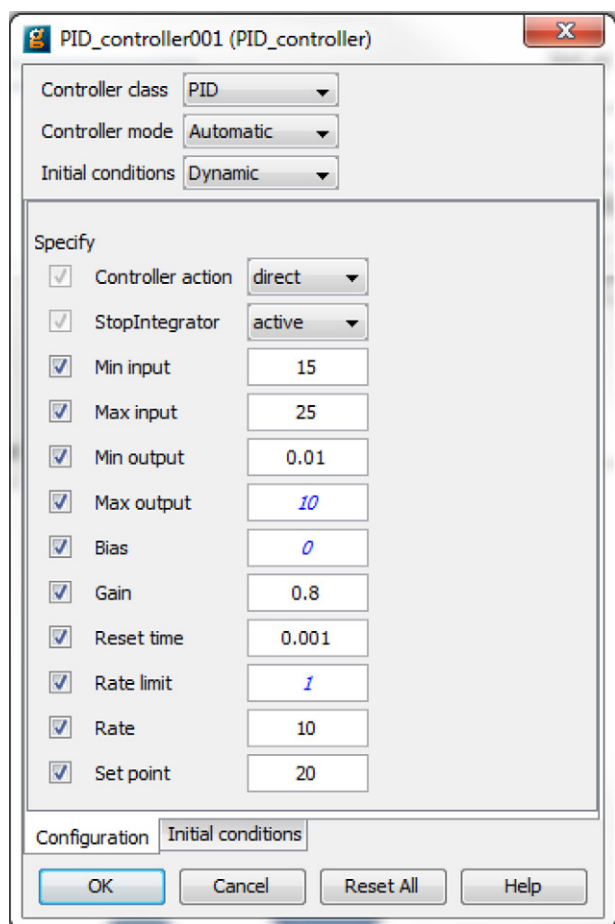**Fig. B.1.** Input control parameters (user interface).

At any time during dissolution, the dissolution of substance i is the summation of substance dissolved from all voxels and can be calculated as follows:

$$des_i = \sum_{j=1}^{n} f_i(1 - \varepsilon) - \phi_i$$

where n is the number of voxels, f_i is the fraction of ith substance, ε is the porosity. With respect to time the dissolution (fraction of the substance dissolved) will increase, therefore the dissolution at certain time (e.g. 30 min) is given as follows:

$$des_i(t_{30}) = \sum_{j=1}^{n} f_i(1 - \varepsilon) - \phi_i(t_{30})$$

A.10.2. Controller model

The deviation from the set point of tablet dissolution is calculated:

$$error_{des} = des(t_{30})_{set} - des(t_{30})_{set}$$

The set point for the slave controller (for hardness) is calculated on the basis of the deviation from the set point of tablet hardness, using a PID control law:

$$H_{set} = K_C^{des}error_{des} + \frac{1}{K_I^{des}} \int_0^t error_{des} \, dt + K_D^{des}\frac{d(error_{des})}{dt}$$

H_{set} is used in F2.2 for hardness control.

Appendix B. Controller specifications

See Fig. B.1.

References

Baumann, M., Baxendale, I.R., Ley, S.V., Nikbin, N., Smith, C.D., Tierney, J.P., 2008. A modular flow reactor for performing Curtius rearrangements as a continuous flow process. Org. Biomol. Chem. 6, 1577–1586.

Betz, G., Junker-Burgin, P., Leuenberger, H., 2003. Batch and continuous processing in the production of pharmaceutical granules. Pharm. Dev. Technol. 8 (3), 289–297.

Blanco, M., Alcalá, M., 2006. Content uniformity and tablet hardness testing of intact pharmaceutical tablets by near infrared spectroscopy: a contribution to process analytical technologies. Anal. Chim. Acta 557, 353–359.

Boukouvala, F., Niotis, V., Ramachandran, R., Muzzio, F., Ierapetritou, M. An integrated approach for dynamic flowsheet modeling and sensitivity analysis of a continuous tablet manufacturing process: an integrated approach. Comput. Chem. Eng., in press, http://dx.doi.org/10.1016/j.compchemeng.2012.02.015

Boukouvala, F., Ramachandran, R., Vanarase, A., Muzzio, F.J., Ierapetritou, M., 2011. Computer aided design and analysis of continuous pharmaceutical manufacturing processes. Comp. Aided Chem. Eng. 29, 216–220.

Buchholz, S., 2010. Future manufacturing approaches in the chemical and pharmaceutical industry. Chem. Eng. Process 49, 993–995.

Charoo, N.A., Shamsher, A.A.A., Zidan, A.S., Rahman, Z., 2012. Quality by design approach for formulation development: A case study of dispersible tablets. Int. J. Pharm. 423, 167–178.

FDA, 2004, Guidance for Industry: PAT-A framework for innovative pharmaceutical manufacturing & quality assurance. 19 June 2012, http://www.fda.gov/downloads/Drugs/GuidanceComplianceRegulatoryInformation/Guidances/ucm070305.pdf

FDA/CDER, 2005. OPS process analytical technology–(PAT) initiative, U.S. Food and Drug Administration, Center for Drug Evaluation and Research, 19 June 2012. http://www.fda.gov/AboutFDA/CentersOffices/OfficeofMedicalProductsand-Tobacco/CDER/ucm088828.htm

Gnoth, S., Jenzsch, M., Simutis, R., Lübbert, A., 2007. Process Analytical Technology (PAT): Batch-to-batch reproducibility of fermentation processes by robust process operational design and control. J. Biotechnol. 132 (2), 180–186.

Hsu, S., Reklaitis, G.V., Venkatasubramanian, V., 2010a. Modeling and control of roller compaction for pharmaceutical manufacturing. Part I: Process dynamics and control framework. J. Pharm. Innov. 5, 14–23.

Hsu, S., Reklaitis, G.V., Venkatasubramanian, V., 2010b. Modeling and control of roller compaction for pharmaceutical manufacturing. Part II: Control and system design. J. Pharm. Innov. 5, 24–36.

i.e. the source term is nil if the ith component is not present in a given voxel as a solid. The diffusion coefficient is related to the overall solids volume fraction via following equation:

$$D_i = D_{i0}\left(1 - \sum_{j=1}^{n} \phi_j\right)^{\alpha_i}$$ (G.3)

This means that diffusivity is zero for a completely solid voxel and equal to the component's bulk diffusivity when the voxel contains only the fluid phase. The parameter ⸜ can be used to account for non-linearity.

The diffusion of each component is coupled with a local change of its phase volume fraction in the tablet via following equation:

$$\frac{\partial \phi_i}{\partial t} = -\frac{S_i}{\rho_i}$$ (G.4)

To solve the model, the tablet has been discretized using cubic volume elements or voxels on a Cartesian grid using phase volume fraction of the tablet solid components $\phi_i \in (0 : 1)$. A volume fraction of unity corresponds to a completely solid voxel whereas voxel of zero contains only liquid phase. Eqs. (G.1)–(G.4) are applicable for each voxel but the boundary initial conditions of outer and inner voxel will be different taking into account that the substance in outer voxel will dissolve before inner the substance in inner voxel.

Huang, Z., Wang, B., Li, H., 2002. An intelligent measurement system for powder flowrate measurement in pneumatic conveying system. IEEE Trans. Instrum. Meas. 51 (4), 700–703.

Kawakita, K., Ludde, K.H., 1971. Some considerations on powder compression equations. Powder Technol. 4, 61–68.

Kimber, J.A., Kazarian, S.G., Stepánek, F., 2011. Microstructure-based mathematical modelling and spectroscopic imaging of tablet dissolution. Comput. Chem. Eng. 35, 1328–1339.

Kuentz, M., Leuenberger, H., 2000. A new model for the hardness of a compacted particle system, applied to tablets of pharmaceutical polymers. Powder Technol. 111, 143–145.

Lamb, G.W., Al Badran, F.A., Williams, J.M.J., Kolaczkowski, S.T., 2010. Production of pharmaceuticals: Amines from alcohols in a continuous flow fixed bed catalytic reactor. Chem. Eng. Res. Des. 88, 1533–1540.

Lomel, S., Falk, L., Commenge, J.M., Houzelot, J.L., Ramdani, K., 2006. The microreactor a systematic and efficient tool for the transition batch to continuous process? Chem. Eng. Res. Des. 84 (A5), 363–369.

Malhotra, G., 2009. Pharmaceutical processing—batch or a continuous process: a choice. Pharm. Process., 16–17.

Matsoukas, T., Kim, T., Lee, K., 2009. Bicomponent aggregation with composition dependent rates and the approach to well-mixed state. Chem. Eng. Sci. 64 (4), 787–799.

Plumb, K., 2005. Continuous processing in the pharmaceutical industry: Changing the mind set. Chem. Eng. Res. Des. 83 (A6), 730–738.

Portillo, P.M., Vanarase, A., Ingram, A., Seville, J.K., Ierapetritou, M.G., Muzzio, F.J., 2010. Investigation of the effect of impeller rotation rate, powder flow rate, and cohesion on powder flow behavior in a continuous blender using PEPT. Chem. Eng. Sci. 65, 5658–5668.

Prats-Montalbán, J.M., Jerez-Rozo, J.I., Romañach, R.J., Ferrer, A., 2012. MIA and NIR chemical imaging for pharmaceutical product characterization. Chemometr. Intell. Lab., http://dx.doi.org/10.1016/j.chemolab.2012.04.002.

Ramachandran, R., Chaudhury, A., 2012. Model-based design and control of continuous drum granulation processes. Chem. Eng. Res. Des. 90 (8), 1063–1073.

Ramachandran, R., Arjunan, J., Chaudhury, A., Ierapetritou, M., 2012. Model-based control loop performance assessment of a continuous direct compaction pharmaceutical processes. J. Pharm. Innov. 6 (3), 249–263.

Roggo, Y., Jent, N., Edmond, A., Chalus, P., Ulmschneider, M., 2005. Characterizing process effects on pharmaceutical solid forms using near-infrared spectroscopy and infrared imaging. Eur. J. Pharm. Biopharm. 61, 100–110.

Saaby, S., Knudsen, K.R., Ladlow, M., Ley, S.V., 2005. The use of a continuous flow-reactor employing a mixed hydrogen flow stream for the efficient reduction of imines to amines. Chem. Commun., 2909–2911.

Schaber, S.D., Gerogiorgis, D.I., Ramachandran, R., Evans, J.M.B., Barton, P.I., Trout, B.L., 2011. Economic analysis of integrated continuous and batch pharmaceutical manufacturing: a case study. Ind. Eng. Chem. Res. 50, 10083–10092.

Seborg, D.E., Edgar, T.F., Mellichamp, D.A., 2004. Process Dynamics and Control, second ed. John Wiley & Sons, Inc.

Sedelmeier, J., Ley, S.V., Baxendale, I.R., 2009. An efficient and transition metal free protocol for the transfer hydrogenation of ketones as a continuous flow process. Green Chem. 11, 683–685.

Sen, M., Ramachandran, R. A multi-dimensional population balance model approach to continuous powder mixing processes. Adv. Powder Technol., in press, http://dx.doi.org/10.1016/j.apt2012.02.001

Sen, M., Singh, R., Vanarase, A., John, J., Ramachandran, R., 2012. Multi-dimensional population balance modeling and experimental validation of continuous powder mixing processes. Chem. Eng. Sci. 80, 349–360.

Singh, R., Rozada-Sanchez, R., Wrate, T., Muller, F., Gernaey, K.V., Gani, R., Woodley, J.M., 2011. A retrofit strategy to achieve Fast, Flexible, Future (F3) pharmaceutical production processes. Comp. Aided Chem. Eng. 29, 291–295.

Singh, R., Raquel Rozada-Sanchez, R., Dean, W., Perkins, J., Muller, F., Godfrey, A., Gernaey, K.V., Gani, R., Woodley, J.M., 2012. A generic process template for continuous pharmaceutical production. Comp. Aided Chem. Eng. 31, 715–719.

Singh, R., Gernaey, K.V., Gani, R., 2009. Model-based computer-aided framework for design of process monitoring and analysis systems. Comput. Chem. Eng. 33 (1), 22–42.

Singh, R., Gernaey, K.V., Gani, R., 2010a. ICAS-PAT: a software for design, analysis & validation of PAT systems. Comput. Chem. Eng. 34 (7), 1108–1136.

Singh, R., Gernaey, K.V., Gani, R., 2010b. An ontological knowledge based system for selection of process monitoring and analysis tools. Comput. Chem. Eng. 34 (7), 1137–1154.

Sorokin, L.M., Gugnyak, A.B., 1973. A method of measuring powder flow rates. Powder Metall. Met. Ceram. 12 (12), 1015–1016, http://dx.doi.org/10.1007/BF00791750.

Stitt, E.H., 2002. Alternative multiphase reactors for fine chemicals: a world beyond stirred tanks? Chem. Eng. J. 90, 47–60.

Trout, B.L., 2007. Next-wave model. World Pharmaceutical Frontiers, 19 June 2012. http://www.worldpharmaceuticals.net/editorials/015_march09/WPF015_nextwave.pdf

Vanarase, A., Alcal, M., Rozo, J., Muzzio, F., Romaach, R., 2010. Real-time monitoring of drug concentration in a continuous powder mixing process using NIR spectroscopy. Chem. Eng. Sci. 65 (21), 5728–5733.

Vanarase, A., Muzzio, F.J., 2011. Effect of operating conditions and design parameters in a continuous powder mixer. Powder Technol. 208, 26–36.

Vanarase, A., Gao, Y., Muzzio, F.J., Ierapetritou, M.G., 2011. Characterizing continuous powder mixing using residence time distribution. Chem. Eng. Sci. 66 (3), 417–425.

Watts, P., Haswell, S.J., 2003. Continuous flow reactors for drug discovery. Drug Discov. Today 8 (13), 586–593.

Wheeler, F., 2009. Pharmaceutical and Fine Chemical Continuous Processing. 19 June 2012. http://www.fwc.com/publications/pdf/ContinuousProcessingFlyer.pdf.